AD-A181 265 AN INVESTIGATION OF TURBULENCE MECHANISMS IN V/STOL UPWASH FLOW FIELDS..(U) GRUMMAN AEROSPACE CORP BETHPAGE NY RESEARCH AND DEVELOPMENT C.. B L GILBERT MAR 87 1/1

UNCLASSIFIED RE-730 AFOSR-TR-87-0603 F49620-85-C-0111 F/G 1/1 NL

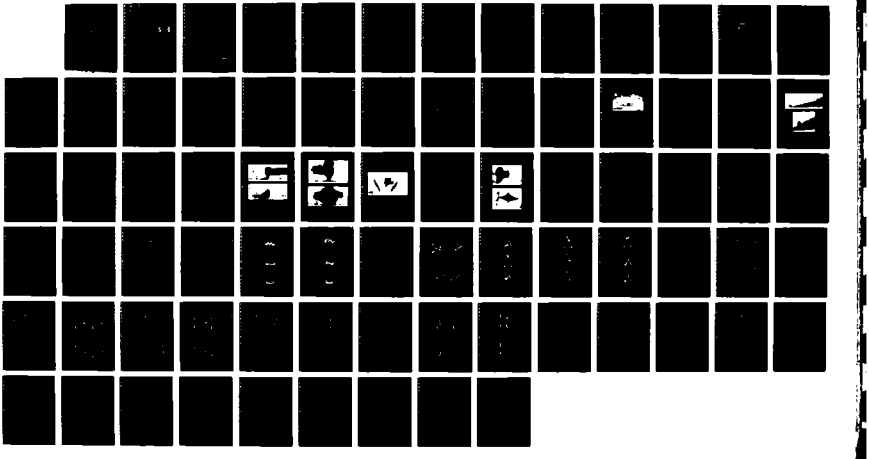

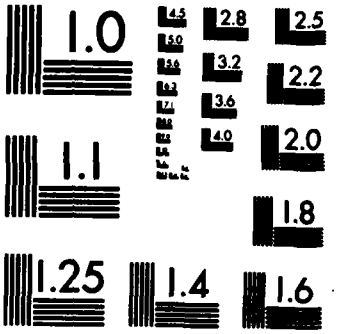


MICROCOPY RESOLUTION TEST CHART
NATIONAL BUREAU OF STANDARDS-1963-A

AFOSR-TR- 87-0603

REPORT RE-730

# AN INVESTIGATION OF TURBULENCE MECHANISMS IN V/STOL UPWASH FLOW FIELDS

MARCH 1987



prepared by

Barry L. Gilbert

Aerosciences Directorate
Grumman Corporate Research Center
Bethpage, New York 11714-3580

Final Report on
Contract F49620-85-C-0111

prepared for

Dr. James D. Wilson
External Aerodynamics and Fluid Mechanics
Air Force Office of Scientific Research
Bolling AFB, Washington D.C. 20332

REPORT RE-730

# AN INVESTIGATION OF TURBULENCE MECHANISMS IN V/STOL UPWASH FLOW FIELDS

MARCH 1987

prepared by

Barry L. Gilbert

Aerosciences Directorate
Grumman Corporate Research Center
Bethpage, New York 11714-3580

Final Report on
Contract F49620-85-C-0111

prepared for

Dr. James D. Wilson
External Aerodynamics and Fluid Mechanics
Air Force Office of Scientific Research
Bolling AFB, Washington D.C. 20332

Approved by: Richard A. Scheuing
Richard A. Scheuing, V.P.
Corporate Research Center

UNCLASSIFIED

SECURITY CLASSIFICATION OF THIS PAGE

ADA181265

## REPORT DOCUMENTATION PAGE

| | |
|---|---|
| 1a. REPORT SECURITY CLASSIFICATION<br>UNCLASSIFIED | 1b. RESTRICTIVE MARKINGS |
| 2a. SECURITY CLASSIFICATION AUTHORITY | 3. DISTRIBUTION/AVAILABILITY OF REPORT<br>APPROVED FOR PUBLIC RELEASE<br>DISTRIBUTION IS UNLIMITED |
| 2b. DECLASSIFICATION/DOWNGRADING SCHEDULE | |
| 4. PERFORMING ORGANIZATION REPORT NUMBER(S) | 5. MONITORING ORGANIZATION REPORT NUMBER(S)<br>AFOSR-TR- 87-0603 |
| 6a. NAME OF PERFORMING ORGANIZATION<br>GRUMMAN<br>6b. OFFICE SYMBOL (If applicable) | 7a. NAME OF MONITORING ORGANIZATION<br>AFOSR/NA |
| 6c. ADDRESS (City, State and ZIP Code)<br>CORPORATE RESEARCH CENTER<br>MAIL STOP A08-35<br>BETHPAGE, NY 11714 | 7b. ADDRESS (City, State and ZIP Code)<br>BUILDING 410<br>BOLLING AFB, DC 20332-6448 |
| 8a. NAME OF FUNDING/SPONSORING ORGANIZATION<br>AFOSR/NA<br>8b. OFFICE SYMBOL (If applicable)<br>NA | 9. PROCUREMENT INSTRUMENT IDENTIFICATION NUMBER<br>F49620-85-C-0111 |
| 8c. ADDRESS (City, State and ZIP Code)<br>BUILDING 410<br>BOLLING AFB, DC 20332-6448 | 10. SOURCE OF FUNDING NOS<br>PROGRAM ELEMENT NO: 61102F; PROJECT NO: 2307; TASK NO: A1; WORK UNIT NO: |
| 11. TITLE (Include Security Classification)<br>(U) AN INVESTIGATION OF TURBULENCE MECHANISMS IN V/STOL UPWASH FLOW | |
| 12. PERSONAL AUTHOR(S)<br>B L GILBERT | |
| 13a. TYPE OF REPORT<br>FINAL<br>13b. TIME COVERED<br>FROM _____ TO _____ | 14. DATE OF REPORT (Yr., Mo., Day)<br>MAR 1987<br>15. PAGE COUNT<br>75 |
| 16. SUPPLEMENTARY NOTATION | |
| 17. COSATI CODES<br>FIELD / GROUP / SUB GR | 18. SUBJECT TERMS (Continue on reverse if necessary and identify by block number)<br>V/STOL, UPWASH, GROUND EFFECT |

19. ABSTRACT (Continue on reverse if necessary and identify by block number)

Results are presented of an experimental investigation of the abnormally high turbulent mixing layer growth rate characteristics found in the upwash regions of V/STOL flows in ground effect. Three dimensional experimental studies were conducted in a radial wall jet facilaty. Measurements included velocity components, second - third - fourth moments, and integral and microscale lengths. The upwash formed by the collision of radial wall jets contains the essential characteristics of a radial upwash while decoupling the problem caused by the impinging jets on the ground plane and the recirculation zone.

Keywords: Vertical Takeoff Aircraft S... Take...

| | |
|---|---|
| 20. DISTRIBUTION/AVAILABILITY OF ABSTRACT<br>UNCLASSIFIED/UNLIMITED ☒ SAME AS RPT ☐ OTIC USERS ☐ | 21. ABSTRACT SECURITY CLASSIFICATION<br>UNCLASSIFIED |
| 22a. NAME OF RESPONSIBLE INDIVIDUAL<br>HENRY E HELIN, CAPTAIN, USAF | 22b. TELEPHONE NUMBER (Include Area Code)<br>202-767-4935<br>22c. OFFICE SYMBOL<br>AFOSR/NA |

DD FORM 1473, 83 APR EDITION OF 1 JAN 73 IS OBSOLETE.

UNCLASSIFIED

SECURITY CLASSIFICATION OF THIS PAGE

## ABSTRACT

Results are presented of an experimental investigation of the abnormally high turbulent mixing layer growth rate characteristics found in the upwash regions of V/STOL flows in ground effect. Experiments were performed in a unique radial wall jet facility to examine the structure of the upwash with the goal of providing qualitative estimates of the momentum distribution and entrainment. This study is the continuation of research utilizing a simpler two-dimensional upwash geometry. The results presented here were obtained using a more complex radial wall jet facility. The unique aspect of the configuration is that the radial wall jets are formed by impinging circular jets coming from below the ground plane onto deflector plates. The upwash formed by the collision of these radial wall jets contains the essential characteristics of a radial upwash while de-coupling the problem caused by the impinging jets on the ground plane and the recirculation zone. Radial wall jet measurements verified traditional values established for mixing layer growth and mean velocity decay. All three velocity components were measured in the upwash as well as second, third and fourth moments; and integral and microscale lengths. Measurements were made at six heights in the centerline plane, at four heights in four planes parallel to the centerline, and in four planes parallel to the symmetry plane. Laser light sheet flow visualization was recorded on video tape. Ground plane pressure contours were measured. Initial parameters used to characterize the upwash formation were identified as the maximum wall jet velocity, and wall jet half-velocity width. The increased mixing layer growth rate was larger than a free jet by a factor of two. This is explained by the much larger eddies and intermittency caused by the head-on collision process at the point where the upwash forms. The time-averaged turbulence level was found to be only about 10% higher than that found in the free jet.

CONTENTS

## LIST OF ILLUSTRATIONS

## LIST OF ILLUSTRATIONS (Contd)

## LIST OF TABLES

# 1. OVERVIEW

A unique turbulent mixing phenomenon results from the collision of opposing wall jets. The mean velocity profile of the generated flow appears to be similar to those found in free and wall jet turbulent flows. However, the macroscopic properties of mixing layer growth rate and the corresponding mean velocity decay rate are significantly different. This combined effect means that there is a different distribution of average momentum in the flow. It is important to properly understand the mixing process and the dynamics of the resulting flow in order to take full advantage of this effect in some applications.

One such flow has recently been identified due to the development of aircraft with V/STOL capability. When a V/STOL aircraft is in ground effect, the exhaust from the aircraft lift jets interacts with the ground, producing an upwash flow directed toward the underside of the aircraft. This upwash flow (including fountains, in the case of more than two jets) has profound aerodynamic implications on the aircraft design by virtue of the additional lift force it imparts to the aircraft at its most critical point of operation, in hover. The induced aerodynamic effects due to upwash augmentation of lift forces and suckdown entrainment over the lower surfaces of only 5% of engine thrust may translate into as much as a 40% difference in mission payload or endurance (Ref 1, 2). An understanding of the basic physical mechanisms acting in the flow field between the aircraft and the ground is vital to the successful development of a practical V/STOL aircraft.

The upwash flow is very difficult to analyze because of the much greater mixing layer growth rate when compared to other types of turbulent flows (Ref 3-10). The problem is made computationally difficult by the intrinsic three-dimensionality of the upwash and because the turbulence in this type of flow is not understood. Numerical codes require better definition of the turbulent structure in order to make reliable predictions of the fountain flow and, later, the fountain/aircraft interaction.

Although the upwash flow field is very complex, the analysis that is most often used is based on a very simple model. The mean velocity profile along a line connecting the source wall jets looks like the profile found in a radial free jet. A simple momentum balance along the collision line requires the

formation of a fan in the symmetry plane between the two jets (see Fig. 1). Extrapolating these velocity vectors back to their virtual origin is equivalent to folding the ground plane down. The flow is then analyzed simply as a radial free jet with its origin located at the impingement point of the source jets. This works fine in the symmetry plane. The most obvious problem with this type of analysis is the much faster growth rate found in the upwash compared to a free jet. This has profound influence on both the distribution of momentum in the upwash and the magnitude of the entrainment field contributing to the suckdown on the aircraft. As diagrammed in Fig. 1, the real upwash fan extends over a much broader region than the free radial upwash model would predict.

This experimental program is designed to investigate the mechanisms that control turbulence levels, mixing layer spread rate, and mean velocity decay rate in the upwash fan, thereby, determining the pertinent scaling parameters of the flow. The goal is to provide a reliable data base for use in predictive computational models and to provide the foundation necessary to properly model the basic V/STOL turbulence equations.

The approach adopted was to initially examine the turbulence found in a very simple two-dimensional flow configuration. The lifting jet impingement region with the ground was eliminated. The radially spreading wall jets were replaced by simple two-dimensional wall jets. Specific characteristics contributing to the high turbulence level and to the increased mixing rate were isolated and identified. In addition the upwash turbulence structure was examined in fine detail, providing a detailed data base for the first time. These results were reported previously (Ref 11-14). In this paper we report on detailed measurements taken in the upwash flow created by the collision of radially flowing wall jets. This configuration more closely approximates the actual V/STOL flow behavior. Detailed surveys of the three velocity components and several of their statistical moments are presented. Profiles have been made through the flow domain of the upwash for equal strength wall jets.

In the sections that follow, we will describe the new flow facility that was designed to generate radial wall jets. The wall jet characteristic will be given. The basic upwash mean and turbulent properties will be presented and compared to free jet and two-dimensional upwash results obtained in an

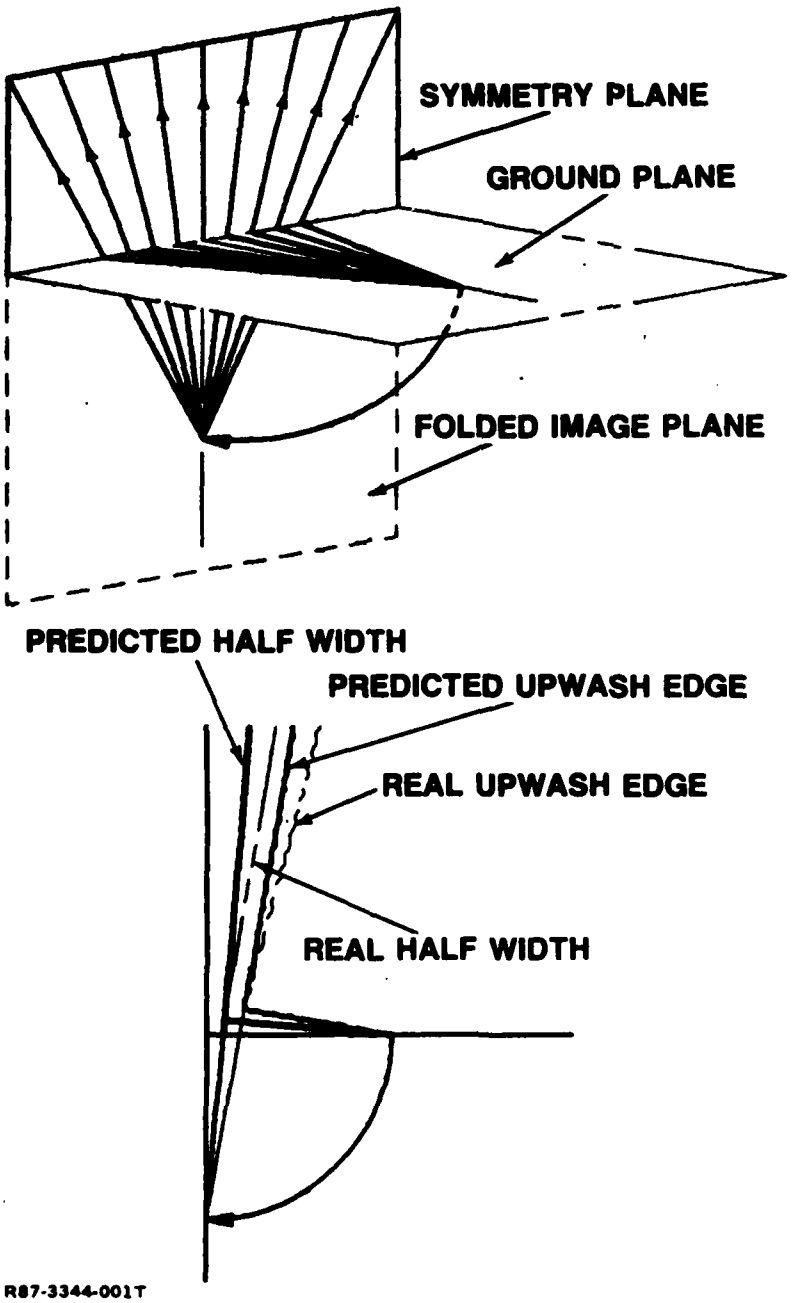


Fig. 1 Diagram Showing Current Analysis Using a Folded Image Plane

earlier investigation. Finally, a discussion of the results and implications to modeling of V/STOL types of flow is given.

# 2. SIGNIFICANT ACCOMPLISHMENTS

## 2.1 BACKGROUND

The data reported in this report represent a continuation of an experimental investigation of the abnormally high turbulent mixing layer growth rate characteristics found in the upwash regions of V/STOL flows in ground effect. The first three years' accomplishments were reported in detail in the three annual reports (Ref 12-14). During the first year's effort, the experimental apparatus used to produce a two-dimensional (2-D) upwash was designed and constructed. After the facility was running and sufficient measurements were obtained to assure two-dimensionality and uniformity of the exit profiles, detailed measurements of the wall jet profiles were obtained. These measurements are very important since these two-dimensional wall jets represent the initial flow conditions for the formation region of the upwash. A single wire anemometer was used to measure one-component mean and turbulence profiles at six locations in the upwash. These measurements provided a comparison set of data to the relatively small sample of upwash measurements that exist in the current literature. These data appear in the first annual report (Ref 12).

The second year's effort included the continuation of the 2-D upwash measurements. Measurements were taken at seven heights between 1 and 8 characteristic lengths in an equal wall jet upwash using an X-wire hot film anemometer. Repeating these measurement positions with the probe rotated 90°, we determined all three velocity components. In addition, higher order turbulent moments were measured. Energy spectra, autocorrelation and cross-correlation measurements, computed with digital fast Fourier transforms, were utilized to determine relevant length scales. While mixing layer growth rates were larger than those found in a free two-dimensional jet, these values were less than those reported by previous investigators. The abnormally high turbulence levels reported by other investigators were not found. These data are presented in similarity form.

Several experiments were conducted to determine the effect of the collision position on the upwash. Using symmetry plates at the position of the collision of equal wall jets, we tested the effects of the stability of the collision point. A study was conducted on the effects of unequal wall

jets on the position and turbulence structure of the upwash. These results are compared favorably to a simple theory. The upwash data can be characterized in a manner similar to the equal wall jet case. Obstacles of various heights were placed at the collision point of equal wall jets. Away from the influences of the obstacle's wake, the upwash exhibited increasing decay rates with decreasing obstacle heights. As expected, this behavior asymptotes to the no-obstacle case for small obstacles and to twice the wall jet growth for large obstacles. These data are reported in the second annual report (Ref 13).

The third year's effort completed the investigation of the 2-D upwash geometry. Initial parameters used to characterize the upwash formation were identified as the maximum wall jet velocity and wall jet half velocity width. Upwash measurements were taken in flows formed from equal wall jets with the same maximum velocities and equal wall jets with the same half widths. Besides increasing the parameter range covered by our baseline data set, these additional tests suggest an explanation for the differences in results obtained by other investigations. These data are reported in the final report (Ref 14).

This year's study extends those measurements taken in upwash formed by the collision of opposed two-dimensional wall jets to an upwash formed from the collision of radially flowing wall jets. The results of this study are summarized here and expanded in the following subsections.

The upwash flow was formed from the collision of two opposing radially flowing wall jets. The wall jets are created in a unique way that allows the upwash to form without any interference due to the source jets. The upwash flow exhibits very large mixing rates compared to turbulent free or wall jet flows. A unique set of two component velocity profiles was taken in the upwash flow field. These measurements include several higher moment terms that appear in the turbulent kinetic energy equations, as well as length scales and intermittency determinations. Measurements were taken along the axis connecting the two source jets as well as off this axis at six measurement stations above ground. The results provide detailed data on an important class of flows where none existed, and they are expected to significantly improve the computational empirical tools available for predicting V/STOL behavior near the ground.

The radial wall jet facility was constructed to create a more complex flow configuration. This facility employs a unique design that creates the radial wall jets from source jets below the instrumentation plate. The upwash formed by the collision of these radial wall jets is not influenced by the presence of impinging jets. As in the two-dimensional case, this allows for the systematic investigation of the upwash phenomenon without the additional complications introduced by the impinging jets and re-circulation zone.

We have used this new geometry to specifically test those parameters that directly affect the upwash growth rate and turbulence structure found to be important in the two-dimensional upwash. We have generated detailed surveys of the three components of velocity and their statistical moments for several types of wall jet collision regions. The interpretation of these data confirm the influence of initial starting conditions on the upwash turbulence characteristics and growth rate. In comparison with existing data by other investigators on similar flows, some of the variation in measured turbulence properties can be explained. It should be pointed out that there is very little data available on even the more general radial free jet flow and almost none on the radial upwash.

## 2.2 APPARATUS AND INSTRUMENTATION

A new wind tunnel facility was designed and constructed for the study of the upwash created from the collision of radially flowing wall jets. The usual method employed for the generation of this sort of wall jet is the impingement of a circular free jet into a ground plane. While this method undoubtedly creates a radial wall jet in the case of an upwash, it also introduces an additional complication. It is impossible to isolate the effects of the presence of circular free jets on the development of the upwash physically located between them. The downward-flowing free jets set up a strongly coupled secondary rotating flow with the upward-flowing upwash.

We wanted to generate a highly controllable upwash flow whose characteristics would not be affected by the presence of a large secondary flow. The geometry chosen was one that employed a circular source jet flowing through the ground plane from below. The circular jet is diverted into the radial direction along the ground by impinging it on a circular deflector plate.

The basic concept of the design is shown in Fig. 2. Several wall jet profiles were obtained from a conventional free jet impingement. These data and established standard radial wall jet data were used to compare the wall jet profiles measured from the various geometries tested. Mean velocity decay curves and wall jet half height growth rate curves were also compared to assure that the wall jet obtained in the new geometry had the same characteristics as a conventional radial wall jet. Tests were conducted at several gap heights and with deflector plates of three different diameters. Decay and growth characteristics were computed from mean velocity profiles taken at the exit and at least six locations downstream.

It was found that if the gap was too large, the wall jet would form on the deflector plate, i.e., it would stick to the wrong surface. An example is shown in Fig. 3. Once this effect was identified, the choice of deflector plates was driven by the desire to minimize the internal diffusion effect as the flow changes direction. The largest radius of curvature supply nozzle available was chosen for the same reason. There is a net diffusion inside the turn if $r^2 < 2RG$. In the small gap case, there is a minimum flow cross-sectional area at the nozzle lip, normal to the plate. There is no net diffusion up to this point, only beyond. A separation bubble at the inner nozzle lip could promote downstream problems on the adjacent wall. In the large gap case, there is a minimum flow area in the nozzle, and diffusion area depends on the gap height. The plate was chosen such that the diffusion of the wall jet flow would take place outside of the turn.

Figures 4 and 5 show the normalized mean velocity decay profiles and half width growth rate for acceptable flow geometries. In this form, the decay is independent of the specific arrangement. However, the effect of the internal diffusion on the flow rate is apparent in Fig. 6. The smaller gaps induce more flow. The smallest gap height was chosen for the full scale apparatus. Our selection was based on the best agreement with classical wall jet characteristics. Figure 7 shows the normalized downstream development of the mean velocity wall jet profiles.

In the literature there are many different geometries used to create a radial wall jet. Most of these use an impinging jet or two constrained circular jets that are made to collide. Those methods seem to have somewhat unpredictable results particularly in the near field. While the spread rate

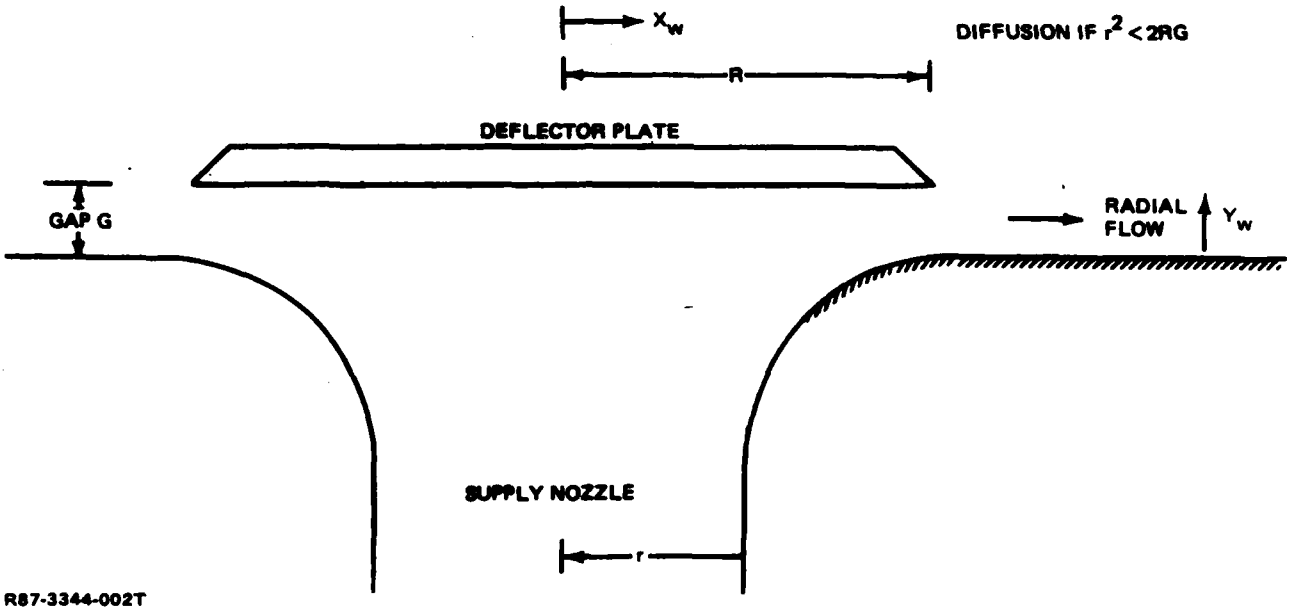


Fig. 2 Diagram of Radial Wall Jet Design

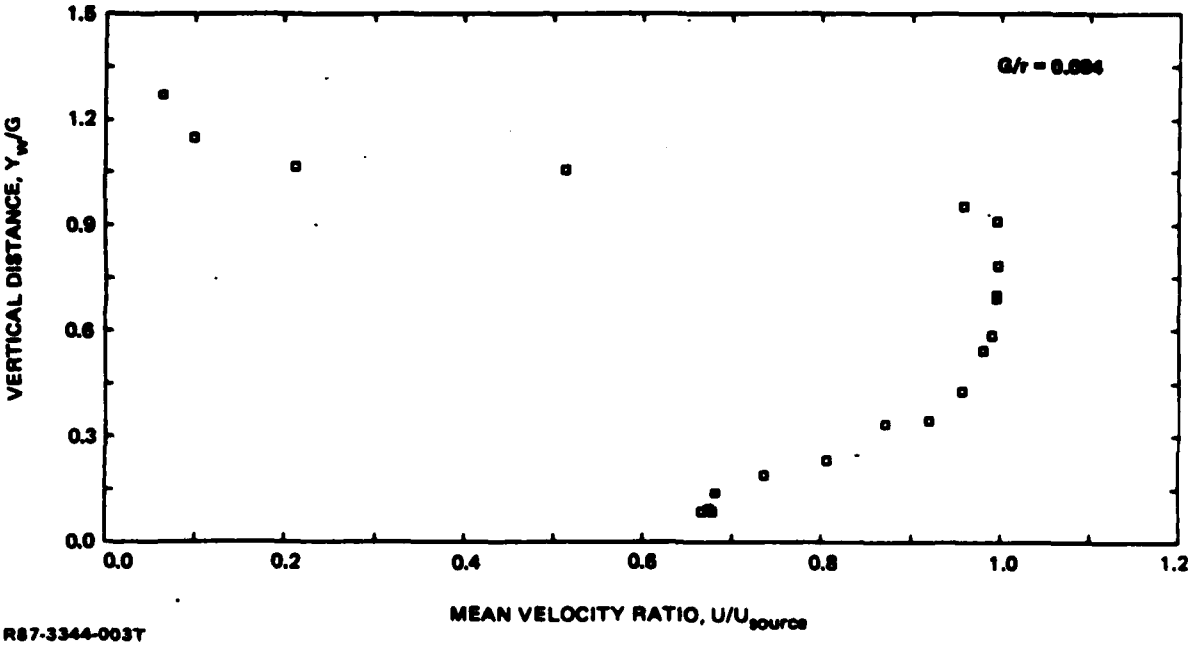


R87-3344-003T
1335-025D

Fig. 3 Radial Wall Jet Exit Profiles

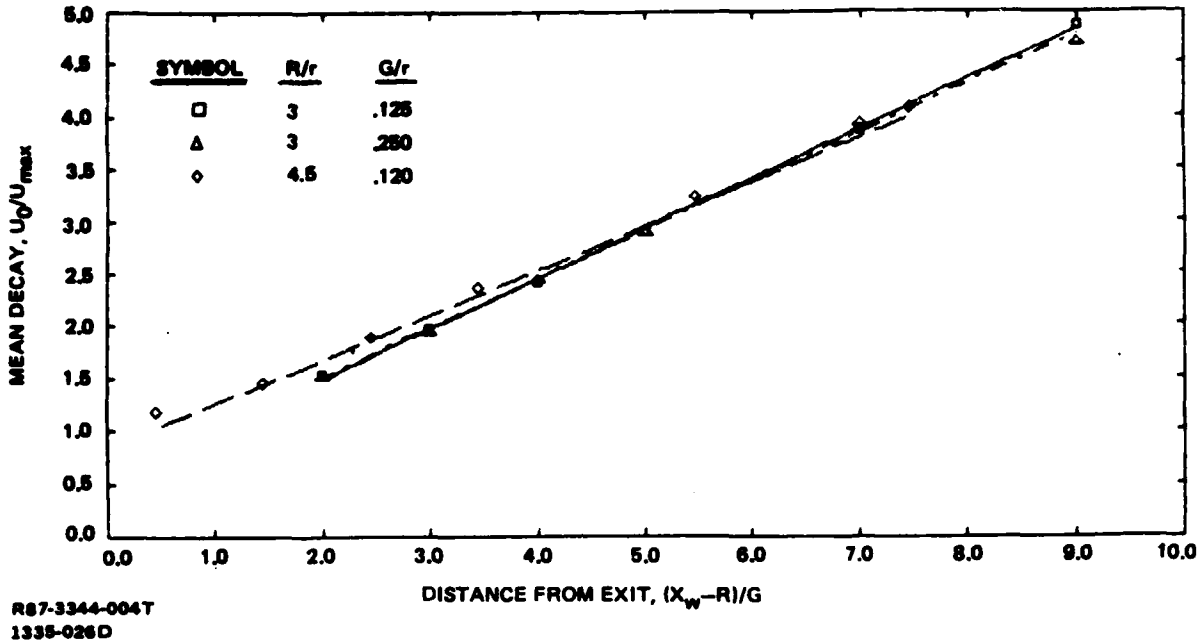


**Fig. 4 Radial Wall Jet Mean Velocity Decay Profile**

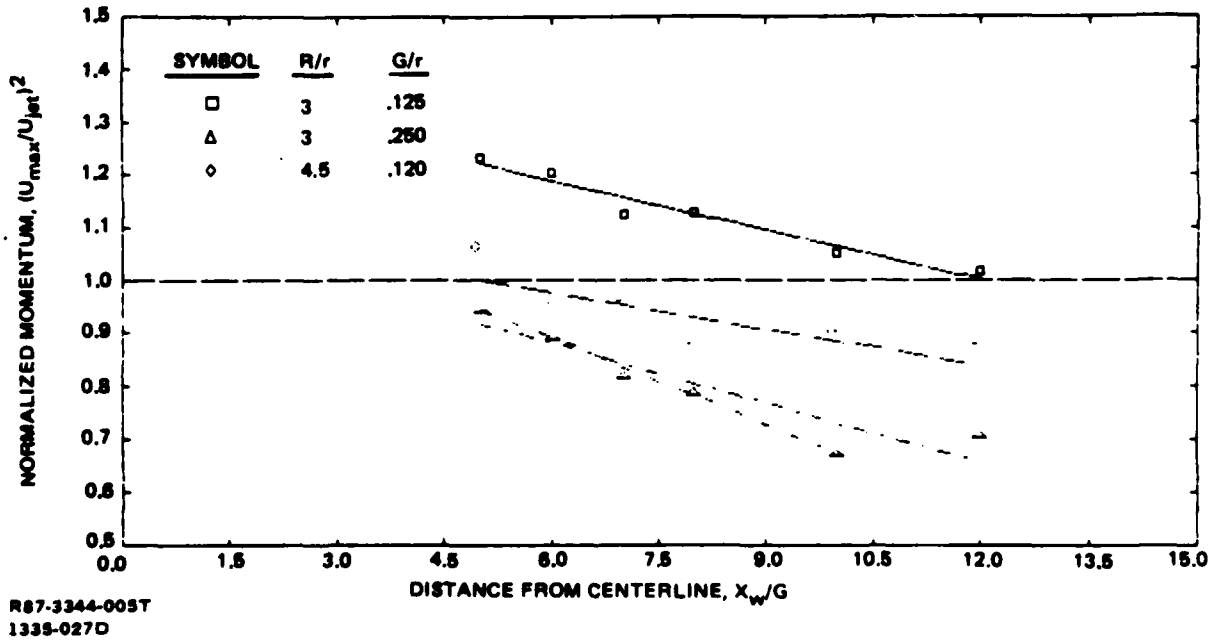


**Fig. 5 Radial Wall Jet Momentum for Different Gap Heights**

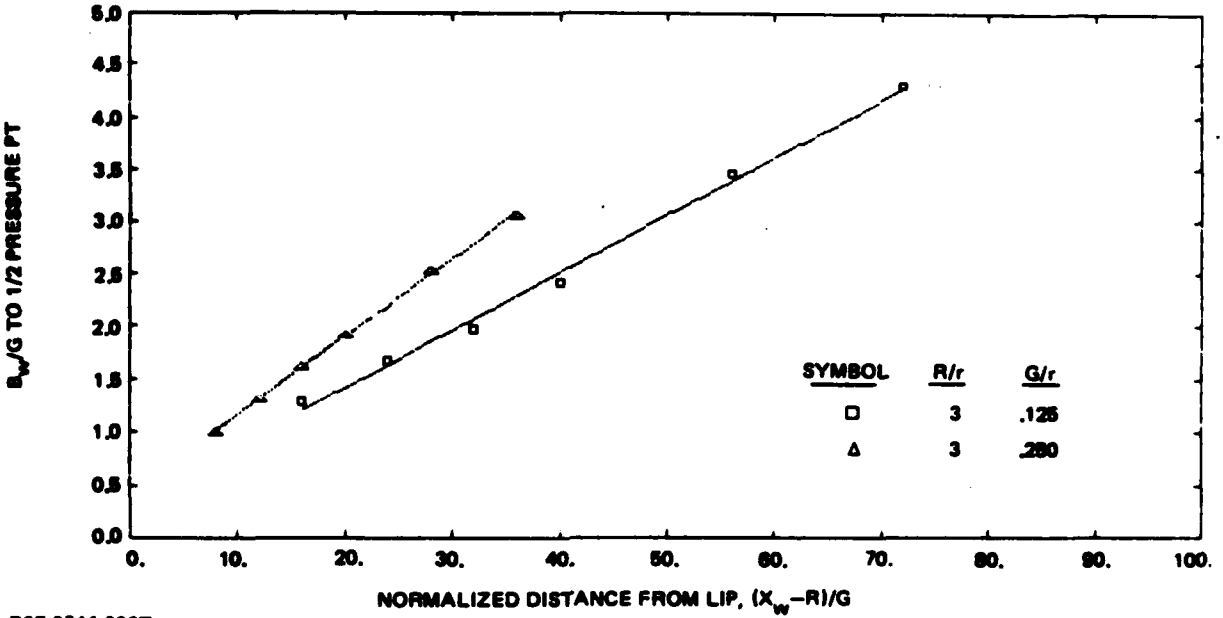


R87-3344-006T
1335-028D

Fig. 6 Increased Mass Flow Rate for Radial Wall Jets

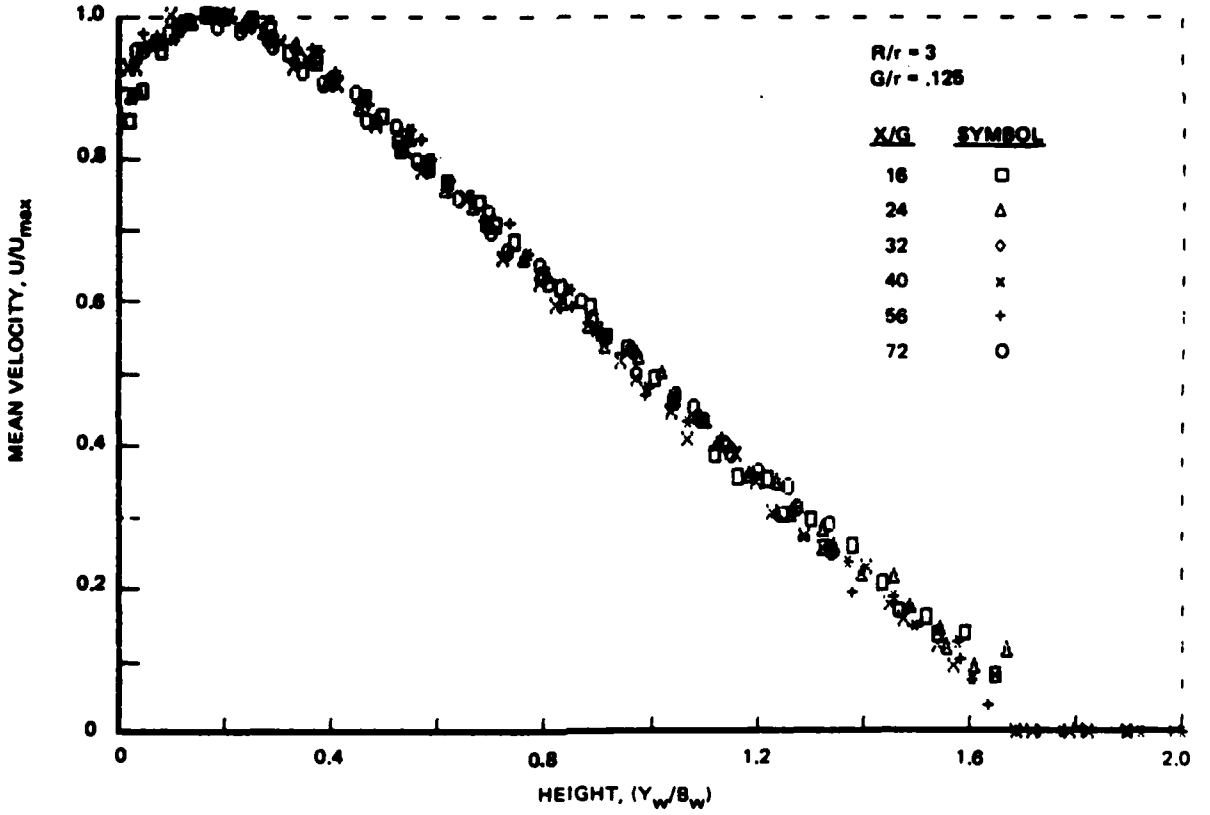


R87-3344-007T
1335-029D

Fig. 7 Radial Wall Jets Mean Velocity Profiles

seems to be relatively insensitive to the method used to generated it, the wall jet requires longer to reach a fully developed flow using a radial nozzle than an impinging jet. The method used here is unique. By varing the deflector cap and gap size it seems to be possible to generate any type of growth rate consistent with conservation laws.

The new flow facility is shown in Fig. 8. The photograph shows the two source jets exhausting from the two independent plenum chambers below the instrumentation plate. The source nozzles are coupled to the instrumentation plate via a flexible collar to provide vibration isolation. The plate is supported by the plenum chambers in such a way as to isolate the flow from any fan vibration that may be transmitted through the chambers. The deflection plates are mounted by three support cantilevers with the gap set by machined spacers. The circular disk in the center contains a series of eight static pressure taps. By rotating this disk, the entire static pressure field between the two source jets may be mapped. The gap height is 5 mm, and the deflection plate has a 15.25 cm diameter. The source nozzle has a 50 cm diameter. The plate is 100 cm x 50 cm, with a jet center distance of 50 cm or 100 gap heights. The radial jet exit velocity is typically 95.5 mps.

The data of this report were taken with a commercial X-probe hot film anemometer calibrated in our facility. The experiment and data acquisition are controlled by our real-time mini-computer system. Two time series from the anemometers and various other flow conditions are taken at each point. The time series are pre-processed in real-time and stored before the program increments the probe position. At each point, 32768 data pairs are taken at 2500 pairs/sec for about 13 sec.

A smoke flow visualization system was used to examine qualitatively the important features of the upwash flow. The system we developed utilized two sets of cylindrical lenses to form a thin laser sheet with variable height and width. An Argon ion laser was used as a source. Two 256 mm focal length cylindrical lenses were spaced nominally 100 mm apart. By adjusting the spacing, laser sheets from 2.5 cm to 25 cm in height could be formed to illuminate whatever flow features we want to examine. Similarly, two 96 mm focal length cylindrical lenses with axes orientated perpendicular to the first set allowed variation in the thickness and sharpness of the sheet. A spacing of about 100 mm gave a very intense sheet at all heights of

approximately 1.5 mm thickness. The laser sheet was moved in space by traversing mirrors on a three axis mechanism. The flow was selectively seeded with one or two smoke sources. The smoke was generated by vaporizing a biologically safe plant oil. The images were recorded on video tape. Photographs were taken from this tape using a digital frame grabber.

A coordinate system was chosen for these experiments that makes it easy to compare new wall jet data with traditional wall jet data, and upwash data with free jet data. A system was chosen that allows the X-direction to be in the direction of the largest velocity component; that is, X is toward the symmetry plane in the wall jets and along the symmetry plane in the upwash. For clarity, wall jet parameters are indicated with a 'w' subscript.

## 2.3 WALL JETS

It is extremely important to fully document the flow characteristics in the radial wall jets. The wall jets are the initial conditions for the upwash. As in any flow, the initial conditions have a tremendous, first order effect on the flow. An upwash is particularly sensitive because it is generated by the head-on collision of wall jets resulting in a stagnation flow with high pressure. Lack of documentation of the initial conditions, i.e., the radial walls jet, seems to be the most serious failing of existing work. Not knowing the starting conditions makes it impossible to compare data. It is like trying to compare free jet data without knowing Reynolds number.

Figure 9 shows typical velocity profiles taken at the exit and slightly downstream of the radial jet, and includes the entrained flow over the top of the deflector plate. Profiles taken at three radial positions around the exit for both jets show very similar profiles. Notice that the flow seems to stick to the deflector plate at the exit but begins to form a normal wall jet profile at only 5 gap heights downstream.

Wall jet mean and turbulence profiles were taken at 16 locations from the jet exit nozzle to a position beyond the instrumentation centerline. The position of these profiles is noted by the numbers along the instrumentation plate shown in Fig. 10. These measurements were made at equal distances along the plate in increments of approximately 4 gap heights. Each profile contains 26 points spanning 12 gap heights. The height is shown by the brackets at stations 15 and 16 in the figure. The data acquisition and movement of the

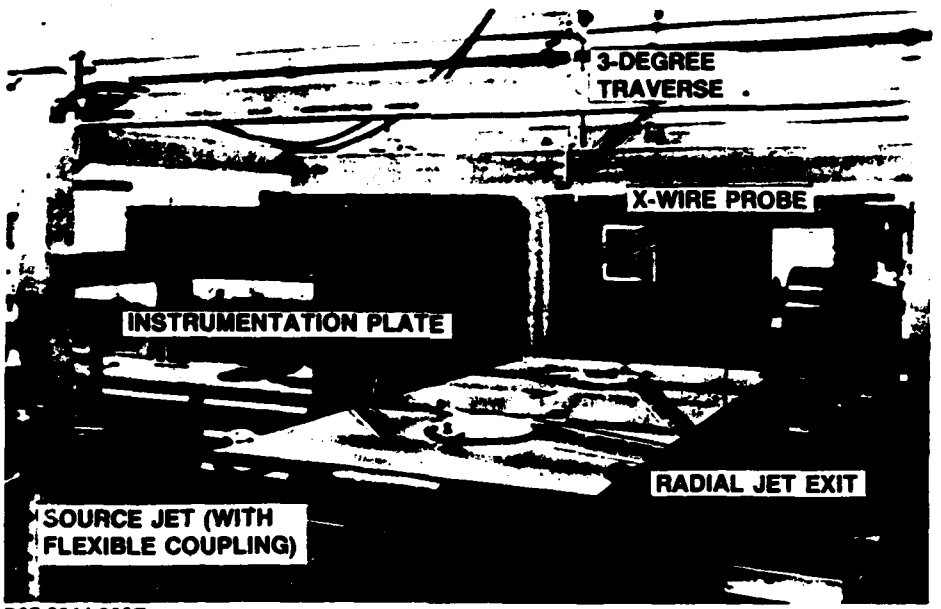


R87-3344-008T

Fig. 8 Photograph of Radial Wall Jet Upwash Facility

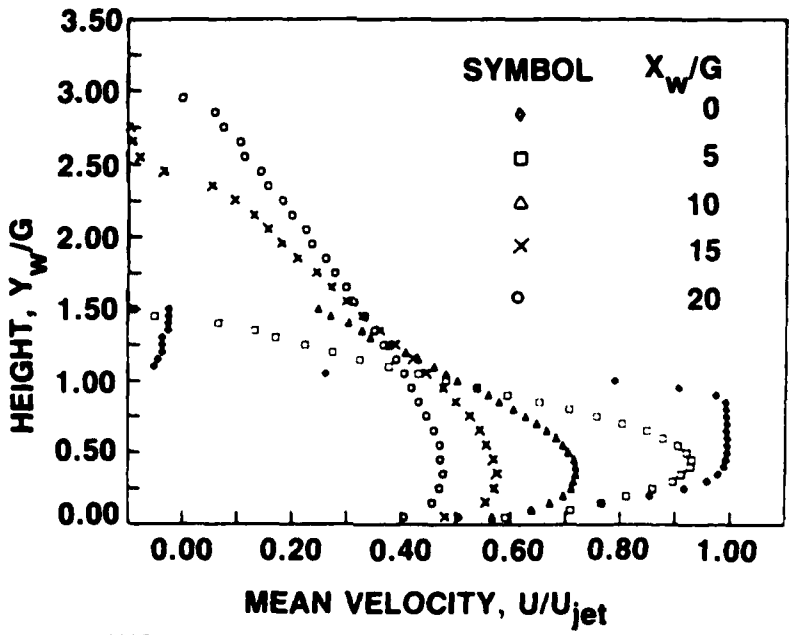


R87-3344-009T

Fig. 9 Typical Jet Exit Velocity Profiles

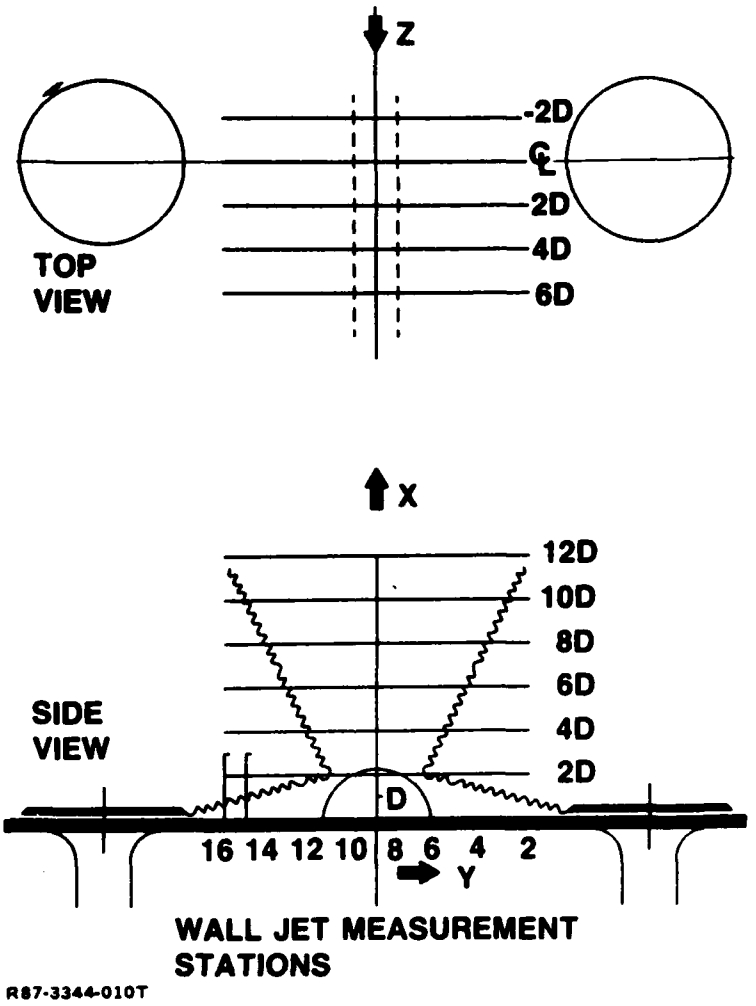


Fig. 10 Diagram Showing Measurement Stations and Coordinate System Used

single-element hot film probe were controlled by the automatic digital data system.

A flow visualization photograph of the radial wall jet is shown in Fig. 11. Figure 11A clearly shows the qualitative behavior expected in a turbulent radial wall jet. The flow is left to right and the seeding is by entrainment with the smoke probe at the radial jet exit. This technique seemed to give very good results. The linear growth of the wall jet can be seen. The dark wedge below the wall jet is the shadow of the right deflector plate in the laser sheet coming from the right. Note the eddy size and apparent intermittency. More of this turbulent structure can be seen in the close up shown in Fig. 11B.

A plot of the wall jet growth rate as characterized by the half velocity height versus the distance downstream is given in Fig. 12A for each wall jet. A linear least squares curve fit of the data from stations 4 through 16 ($X_w$/Gap > 14 to 60) gives a growth rate of 0.097. The first stations were not used in the curve fit because they are in the developing region. Figure 12B shows the linear decay of the maximum velocity versus distance. This relationship is required by conservation of momentum considerations. The data were normalized by the characteristic half height dimension and alternate profiles were plotted. Figure 13 shows that the mean velocity similarity exists as early as $X_w$/Gap = 13, much sooner than usual. The turbulence energy profiles show similarity at about $X_w$/Gap = 20.

The generally accepted growth rate value for an axisymmetric wall jet is 0.078. However, wall jets produced by impinging circular jets on a plate give a value of 0.087, and that value seems to be independent of the height of the impinging jet from the plate. The virtual origins, defined by the half velocity growth curve, are -7.14 and -7.20 gap heights which are about half-way between the geometric centerline and the exit.

The flow rate at any radius can be computed $Q/Q_o = \int U \times dy/U_o RG$. Then for

$$B_w = C_2 x \tag{1}$$

$$U_{max}/U_o = C_1/(\tfrac{X}{G}) \tag{2}$$

and

a)

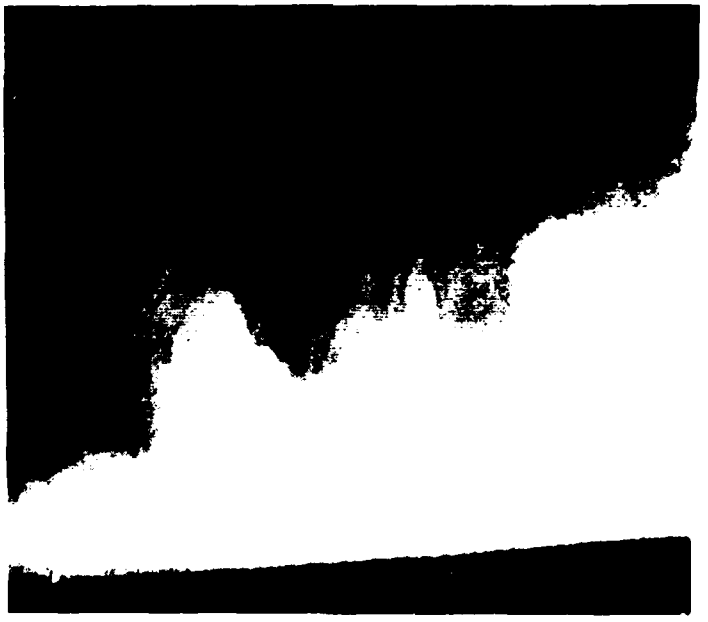

b)

R87-3344-021T

Fig. 11 Flow Visualization Photograph Showing a Single Wall Jet

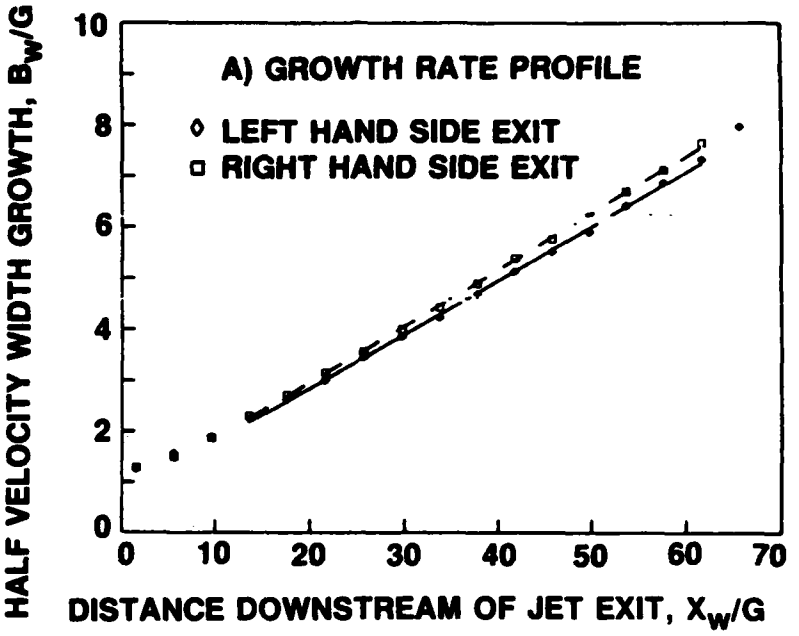


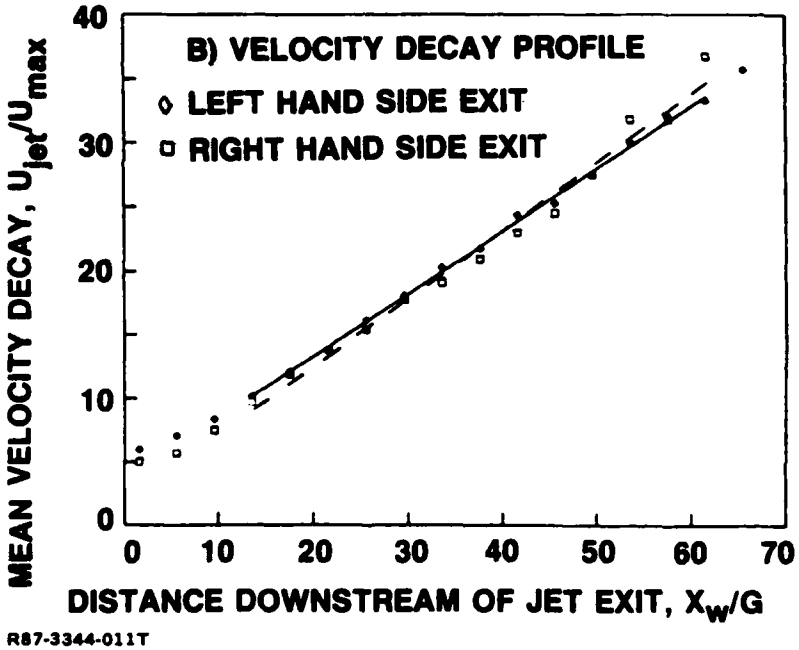


R87-3344-011T

Fig. 12 Radial Wall Jet Characteristics

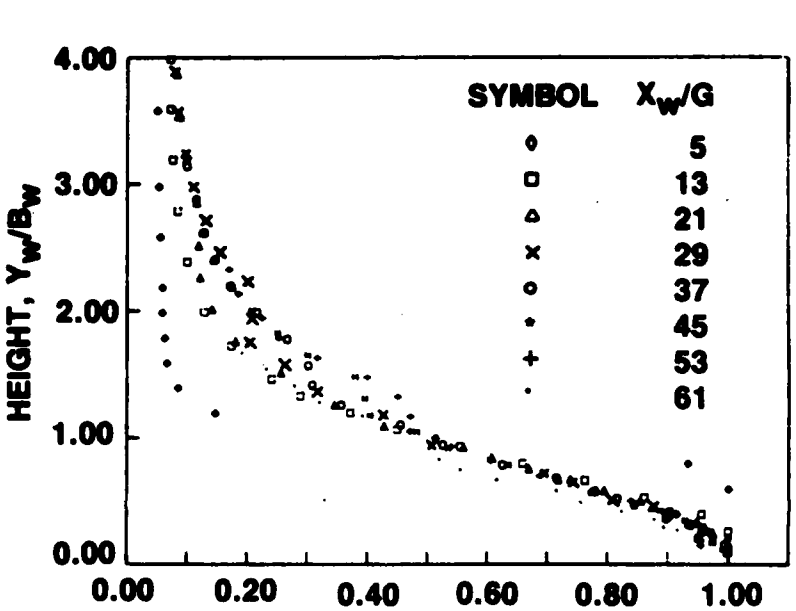


Fig. 13 Radial Wall Jet Mean Velocity Profiles in Similarity Form

$F = \int \frac{u}{u_{max}} d\left(\frac{y}{\delta}\right) = 1.04$ for a normal wall jet velocity distribution gives

$$Q/Q_o = C \left(\frac{X}{R}\right) \tag{3}$$

where

$$C = C_1 C_2 F. \tag{4}$$

The entrainment coefficient can now be estimated from the decay and growth relations using conservation laws and assuming that the entrainment velocity is a constant fraction of the local maximum velocity. For $v_e$ the entrainment velocity at any radius $\alpha_e = v_e/U_m = F\ C_2$. Classical results using $C_1 = 6.85$, $C_2 = 0.078$ gives $C = 0.556$ and $\alpha_e = 0.081$. Values of $C_1$ can range from 5.5 to 9.6. Using my empirical values of $C_1 = 9.33$ and $C_2 = 0.097$ give the values $C = 0.95$ and and $\alpha_e = 0.10$. Lower values of C have been found when the velocity distribution at the exit was not uniform as was the case here. The good comparison of these empirical coefficients justifies the use of this technique to generate realistic turbulent radial wall jets.

Similarly a momentum balance maybe formed as

$$\int U^2 \times dy/U_o^2\ RG \tag{5}$$

reduces to a constant,

$$C_1^2\ C_2\ F_2\ \frac{G}{R} \tag{6}$$

where $F_2$ is the wall jet momentum shape factor = 0.71. Some results give this constant = 0.346 but here the constant = 0.81. The differences between this value and unity is due primarily to the presence of an exit shape factor.

Matching the maximum velocity values at the physical centerline alone was not enough to ensure that the upwash fan would form vertically. In early tests, the matched maximum velocity criterion produced an upwash fan that formed at the physical centerline but that was not vertical. Careful measurement of each velocity profile at the centerline showed that due to almost imperceptible variations in the nozzle exit geometry, one flow had an

excess of momentum above the maximum velocity point. This caused the flow to slant away from that side showing the strong sensitivity of the flow to very small differences in the velocity profile. The source wall jets were manipulated to give nearly identical profiles; therefore, momentum distributions at the collision point also were nearly identical. The exit velocity was 95.5 m/sec which gives a Reynolds number based on jet velocity and nozzle gap height of $33 \times 10^3$.

The wall jet characteristics at the centerline may be determined at $X_w$/Gap = 50. The wall jet parameters when no collision occurs should be used to normalize upwash data in a manner similar to using the wall jet nozzle height and source jet velocity as characteristic parameters in a wall jet flow. At the centerline, the wall jet half velocity height is $B_w$ = 4.0 Gap = D = 20.50 mm, and the characteristic velocity is $U_{c\ell}$ = 0.218 $U_{jet}$ = 20.8 mps. The value D now becomes the characteristic height for the upwash and is used to determine all the measurement stations in the upwash. The collision region of influence extends to about 2D. This is shown as a semi-circle in Fig. 10. The upwash Reynolds number based on these centerline dimensions is $29 \times 10^3$. The distance between source jet geometric centers is 24.8D and between virtual centers is 20.9D.

## 2.4 UPWASH MEASUREMENTS - CENTERLINE

A good qualitative indication of what is happening in the upwash is obtained from the flow visualization picture of the upwash. In Fig. 14 only the left jet is seeded so it is the only one visible. The radial wall jets collide at the centerline creating the upwash. The presence of the right wall jet is clearly visible by its effect on the seeded jet. It appears that no flow emanating from the left passes through to the right hand side of the upwash. The cloud seen to the right in Fig. 14A is due to the seed falling back through the laser sheet coming from the right. The full upwash is made visible in Fig. 15. The relative size of the eddies in the wall jet and the upwash is clearly seen. The less dense smoke outside the upwash structure shows the entrainment flow. Flow is strongly entrained into the base of the upwash as seen by seeding the entrained flow in Fig. 16 . The smoke is ejected from the probes with no velocity of its own. Therefore, the strong suckdown of the entrainment field is due to the presence of the upwash. This is significantly different from a free jet where the smoke would move upward

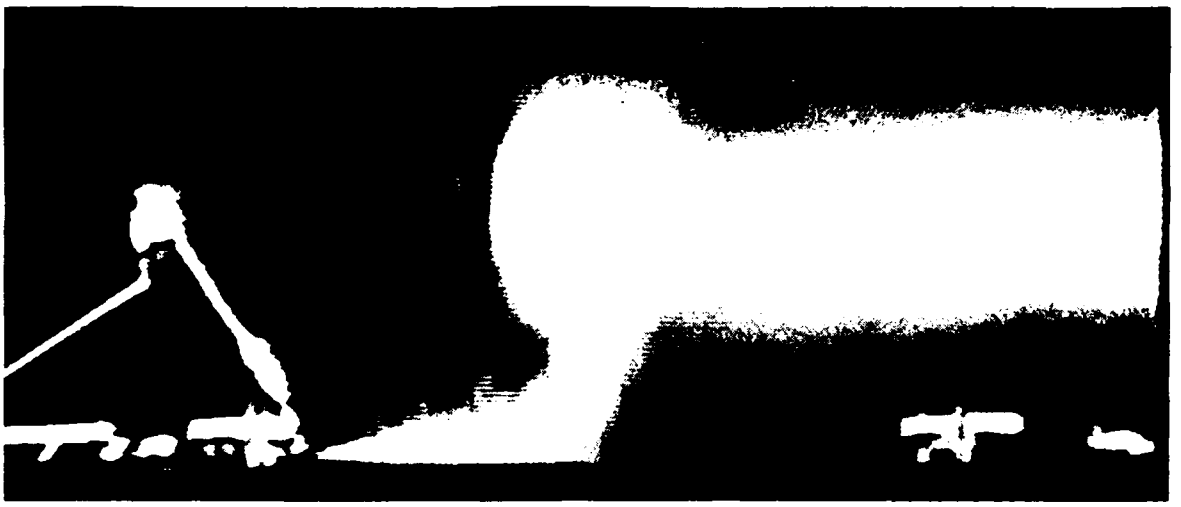

a)

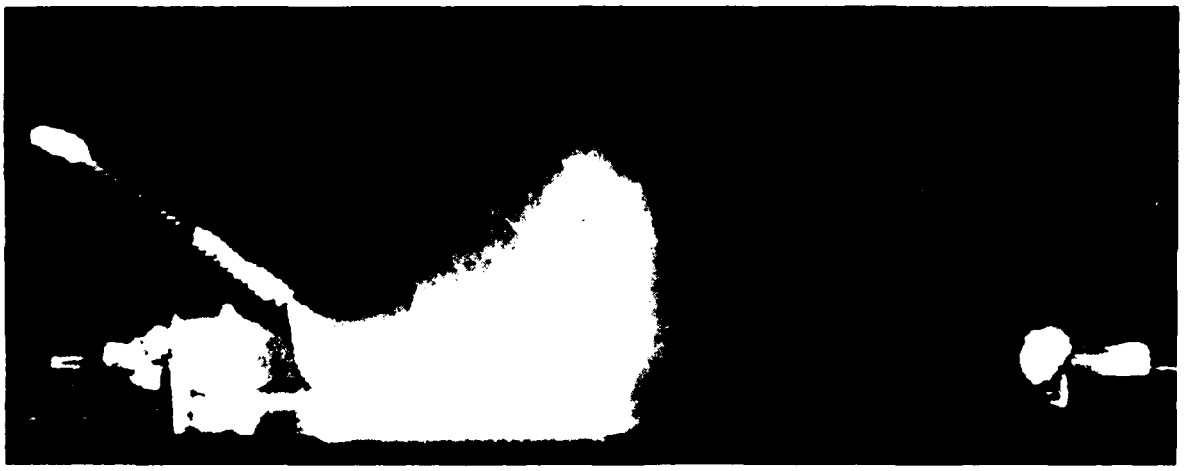

R87-3344-022T

b)

**Fig. 14 Flow Visualization Photograph Showing the Wall Jet Deflection Due to the Upwash Collision**

a)

R87-3344-023T

b)

Fig. 15 Flow Visualization Photograph Showing Full Upwash Structure

R87-3344-024T

Fig. 16 Flow Visualization Photograph Showing Large Entrainment (Suckdown) Flow Field

with the jet, joining it nearly tangentially.

Figure 17 shows these effects again viewed from the top. The laser sheet was rotated 90° so that it illuminated a plane nearly parallel to the ground plane. In fact, the laser plane is at a slight angle to avoid a shadowing problem from the right hand side deflector plane and supports. The bright spots are primarily due to laser light reflections from solid structure. Figure 17A corresponds to Fig. 14 where only the left hand side wall jet is illuminated. Since the seed is injected at a point, a radial pie slice shows up in the laser sheet. Because only one wall jet is seeded but both are running, the flow at the collision point turns abruptly vertical and moves out of the laser plane. No seed penetrates past the collision point at this height above ground. Figure 17B shows both jets seeded, corresponding to the views shown in Fig. 15. The dark horizontal line through the field is a shadow. The laser sheet was also positioned parallel to the symmetry plane with some interesting visualizations. None of these are shown here.

Figure 10 shows the location of the measurement stations in the upwash. The value D, the half velocity height at the collision point of an individual radial wall jet, is the characteristic dimension of the upwash. Measurements were made along the centerline connecting the two jets at 6 heights from 2D to 12D. Measurements at 12D may have been affected by the presences of the probe transverse mechanism and support structure. Profiles also were taken at four cross-stream locations in the Z-direction. These profiles at 2D increments were 6D to -2D and at the same four lower heights used for as the centerline position. Additional profiles were taken along the Z-plane in the symmetry plane and at one-half width to either side of the symmetry plane at heights of 4D and 6D. Each profile contained 60 points positioned approximately 0.23D (4.8 mm) apart, except at the lowest station where they were at half that value. Each profile was repeated with the X-probe rotated 90 degrees so that all three velocity components at each point were measured. Since this procedure repeats the "U" measurement, it is a good check on the reproducibility of the data.

There are two forms of data acquisition programs. These programs are responsible for taking the real-time data, performing some pre-processing, storing the processed data, and controlling the probe movement and timing. The longer form of the program does a complete turbulence analysis; the other

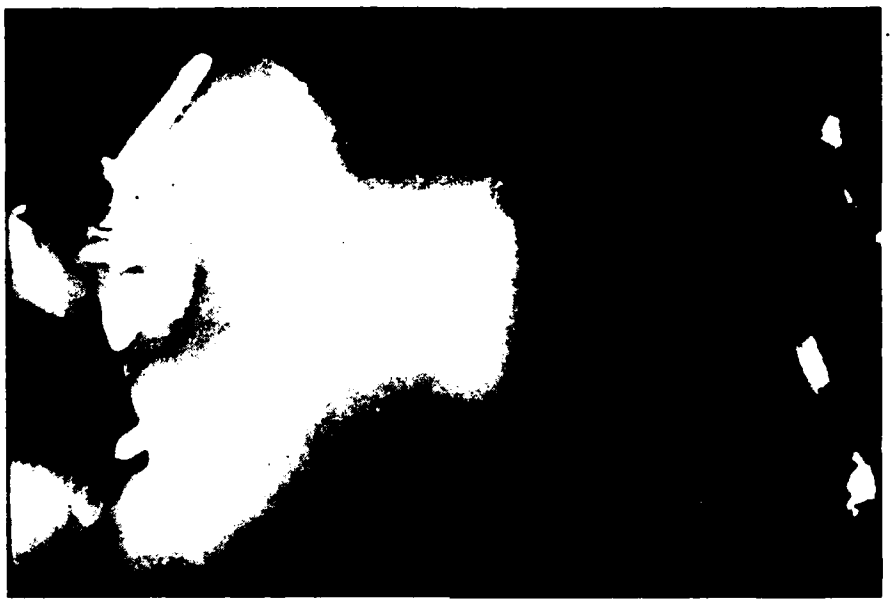

a)

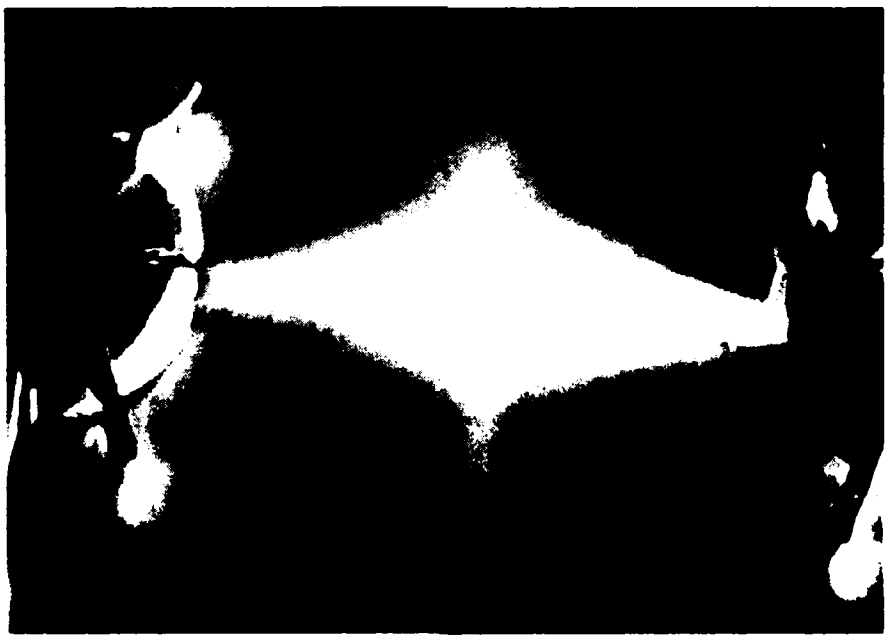

b)

R87-3344-025T

**Fig. 17 Flow Visualization Photograph Showing Single Wall Jet and Both Wall Jets Colliding As Viewed from Above**

computes only means, turbulence energy, and one component Reynolds stress. The long form computes, in addition, third and fourth moments, auto-correlations and cross-correlations, Taylor microscales, and integral scales. These allow calculation of various terms in the turbulent kinetic energy equation, and intermittency. The length scales are calculated by computing the turbulence energy spectra from the time series by using fast Fourier transforms and then computing the correlation using the inverse transform. The Taylor scales also were computed from the derivative of the time series for comparison. Taking time derivatives inherently adds noise so that these values are not as reliable as those obtained from the correlation method. The values agreed well at the symmetry plane where the intermittency is one. Along the centerline, a complete data analysis was done. At all other points off the centerline, a shorter analysis was performed that gives only the first and second moments (means, turbulence energy, and Reynolds stress).

The mean velocity profiles in the upwash direction were curve fit with a least squares curve of the form $U = A+C \exp [-(Y-Y_0)^2/2S^2]$, where $Y_0$ is the symmetry coordinate, A+C is the maximum velocity, and S may be used to define the half velocity width as $B(U=U_{max}/2) = 1.177\ S$. This curve fit procedure is superior to the usual determination of half width that relies on interpolating between data points to find $U_{max}/2$. That method suffers severely from data scatter in both the determination of $U_{max}$ and the interpolation at $U_{max}/2$, and rarely gives symmetric half velocity positions.

The half velocity growth rate curve defined by the curve fit technique is shown in Fig. 18A. The growth rate shown is about 0.25. This value is essentially the same one found in the previous two-dimensional upwash (0.23) and is more than twice the free jet value (0.11). The mean velocity decay curve is shown in Fig. 18B. The data are plotted in a form to give the linear relationship required by conservation of momentum considerations.

The normalized mean velocity profiles at six heights are shown in Fig. 19. The profiles have been shifted to their symmetry point and normalized by the local half velocity width and local maximum mean velocity as determined by the curve fit. It was found in the two-dimensional wall jet studies that the zone of influence of the collision is on the order of two characteristic length scales D. As in that case, there is still some evidence of the turning

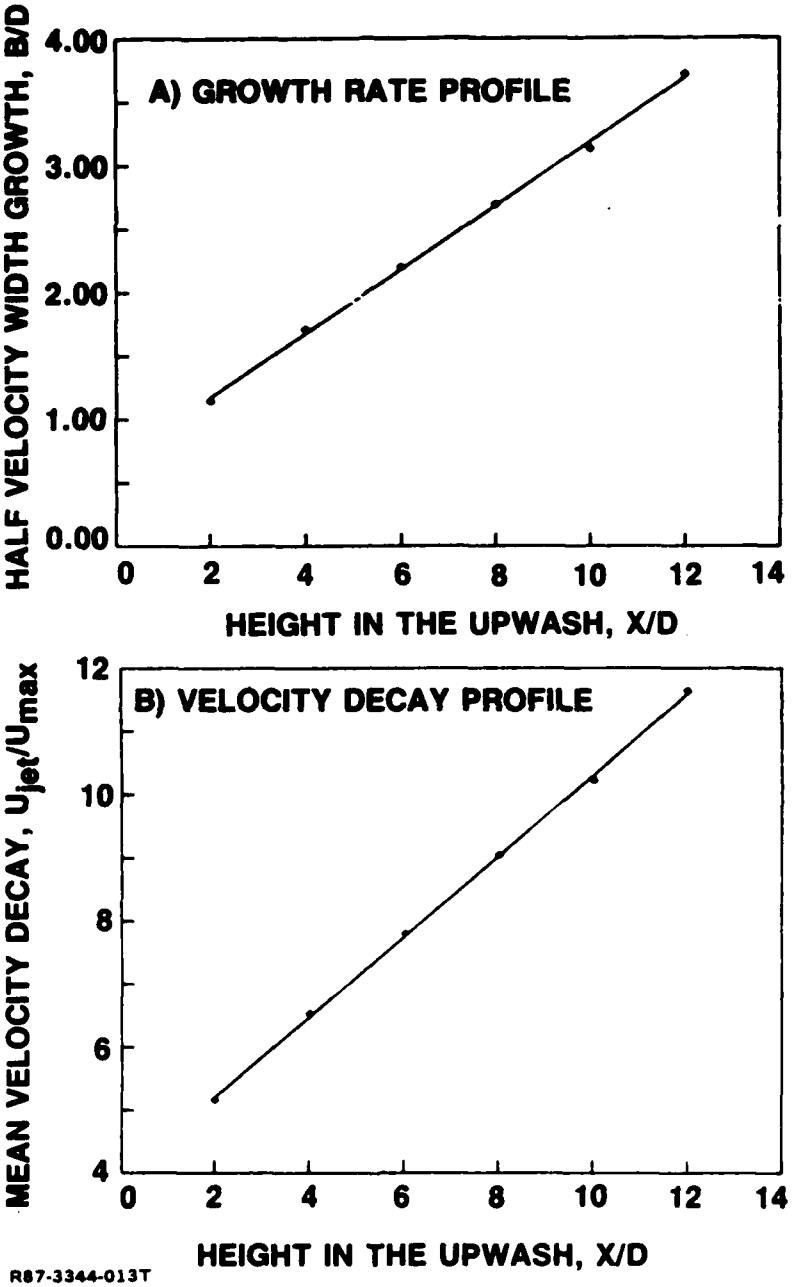


Fig. 18 Radial Upwash Characteristics along the Centerline

of the flow at X/D = 2. The residual velocities shown in the tails of the velocity distribution are similar to those found previously. This entrainment flow is also very evident in the smoke flow visualization studies (Fig. 15). The mean velocity profiles are symmetric. These similarity profiles may be expressed as $U/U_{max} = \exp\{-0.693\ \eta^2\}$ where $\eta = Y/B$. The constants in the curve fits have been absorbed into the virtual origin shift. However, the mixing layer growth rate is about twice the free jet value. The similarity profile for this flow can be written as $U/U_{max} = \exp(-12.0\ (Y/X)^2)$ where the free jet coefficient is between 70.7 and 75.0. Since the mixing layer growth rate is higher, conservation of momentum demands that the mean velocity decay must be correspondingly lower. Our decay curve is $U_{max}/U_o = 1.5/(X/D)$ compared to a coefficient of about 3.5 in the free jet case.

Following an analysis like one used for the radial wall jets, the mass flow rate at any point may be given by

$$Q/Q_{CL} = \int u\ 2\pi\ x\ dy/U_{CL}\ D\ X_{CL}\ 2\pi F \qquad (7)$$

where the denominator represents the mass flow at the centerline from a single wall jet. Using the definitions given before and the empirical data at the centerline gives

$$Q/Q_{CL} = C\ \frac{x}{D} \qquad (8)$$

where

$$C = .438\ C_1 C_2\ \frac{F_2}{F} \qquad (9)$$

$F_2$ = shape factor for the radial free jet = 1.065 and the empirical constant is from the centerline conditions. In this case, C = 0.177 but the entrainment velocity $\alpha_e = 0.27$. This is more than twice 0.12 value found in free radial jets. In the two-dimensional upwash case, the entrainment rate was only 0.125 of the local maximum. As in the radial data given here, this represents an entrainment rate that is 2.4 times a two-dimensional free jet. The entrainment velocity represents only the magnitude of the velocity carrying mass into the upwash and is not expected to appear strictly as a transverse velocity component. The momentum coefficient may again be computed

from

$$\int U^2 \times dy/U_o^2 \; RG \tag{10}$$

gives a constant,

$$1.63 \; C_1^2 \, C_2 \tag{11}$$

While there are some errors in assumptions and calculation of shape factors, evidently they must be compensating because evaluating the above constant with my data gives the constant = 1.01.

In addition to growth rate, another significant departure from free jet characteristics is found in the intermittency. Figure 20 shows the normalized intermittency. The intermittency is determined by the flatness factor normalized by the centerline value. An intermittency factor of one indicates fully turbulent flow. The form of these curves is the expected normal distribution. However, in all free shear flows, the ratio of the intermittency half width to mean velocity half width is two (Ref 15). Our measurements in the upwash give this ratio as one. Again, this statement is limited by the lack of radial free jet data. There is evidence (Ref 3) that a radial free jet intermittency will continue to erode the core for great distances downstream. The data here shows the intermittency structure to be established rapidly and maintained downstream. All profiles of turbulent quantities that we will show will be normalized by local mean velocity half widths. So, while the form of these profiles will look absolutely correct (i.e., like a free radial jet), the widths of the profiles will actually be about twice the free jet widths. Because of the method of normalization, this means that the intermittency profile is really very similar to the free jet profile. Because the upwash intermittency profile does not have a flat region at the centerline, the non-turbulent flow outside the upwash is penetrating nearly to the centerline; that is, the mixing layer must have a penetration length scale nearly equal to the half velocity width. An indication of the size of these eddies compared to a wall jet, for example, can be clearly seen in the flow visualization photographs.

The component turbulence energy in the mean flow direction is shown in Fig. 21A. Similarity is reached at about X/D = 4, which is much faster than

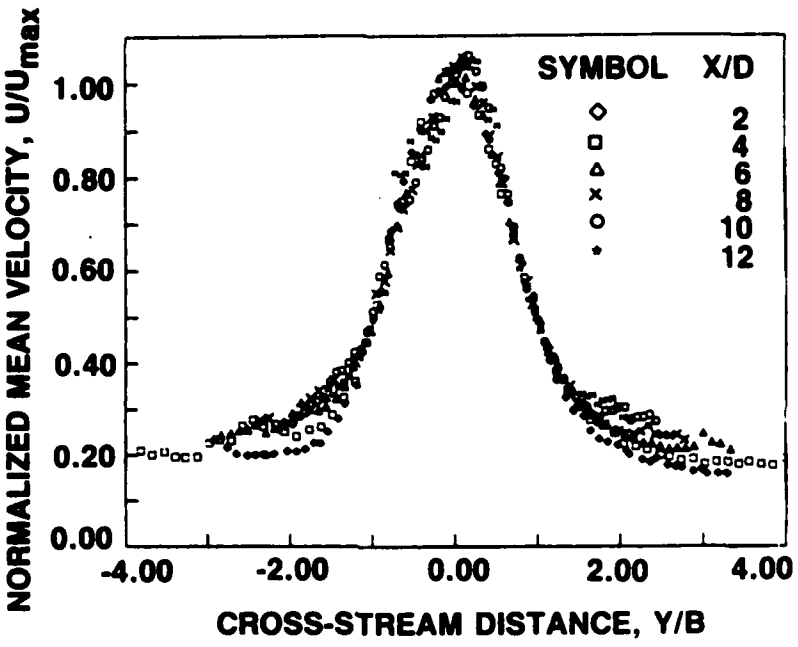


**Fig. 19 Mean Velocity Profiles for a Radial Upwash at Six Heights in Similarity Form**

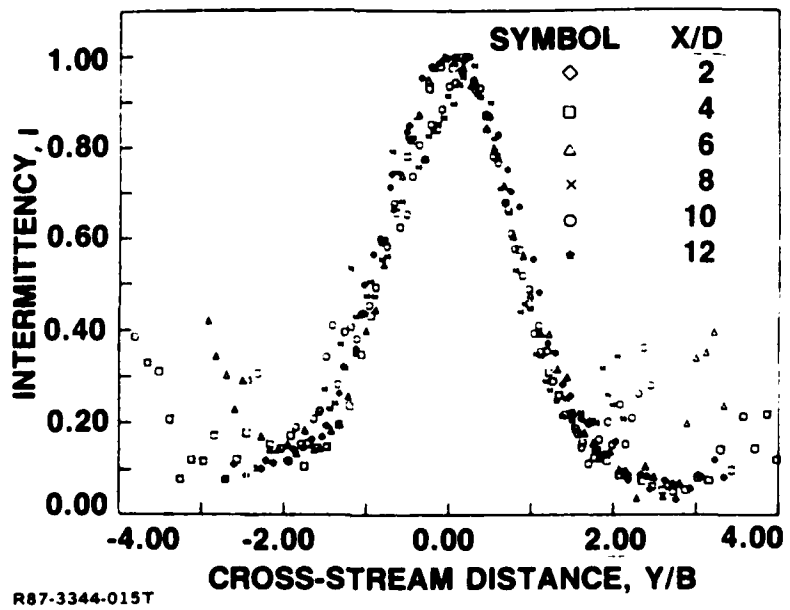


**Fig. 20 Intermittency Profiles at Six Heights**

usually found in radial free jets and is about the same found for the two-dimensional upwash. This may be due to the fact that there is no core region that needs to decay before the similarity jet can form. These profiles are normalized in a manner similar to the mean profiles. The form of these profiles are exactly those expected to be found in a radial free jet but the magnitudes are about 10% high. These turbulent velocity profiles are symmetric and have symmetric peaks. The components in the two cross-stream directions, obtained by rotating the probe, are shown in Fig. 21B and 21C. These two figures show the expected forms and values. The abnormal data at the lowest station, X/D = 2 is because the flow is still turning. Figure 22 shows the total turbulence kinetic energy profile at six measurement stations normalized as before. The total energy $q^2$ reaches similarity quite rapidly, showing that the slower development of the individual components is really due to a redistribution of turbulence among the various components as they approach local isotropy. Examination of the component turbulence energy and total kinetic energy levels found in the upwash shows these values to be approximately the same as those found in ordinary radial jet flows and larger than those found in two-dimensional free jet flows.

Figure 23 shows one component of the Reynolds stress, $\overline{uv}$. Across the center region, the Reynolds stress profiles are anti-symmetric about the centerline passing through zero but have the different magnitudes on either side. Analysis of these data is made difficult by the lack of even good radial wall jet data. There does not seem to be any reliable upwash measurements of higher order quantities. The magnitude and position of the peak Reynolds stress corresponds to values normally calculated for radial free jets. The lower values correspond to values normally measured in radial free jets. It is not clear why there is this discrepancy between theoretical and experimental values. It may have something to do with the large intermittency profile. The difference in magnitude is probably due to the slight angle that the upwash makes with the ground that appears at higher stations. Since Reynolds stress measurements are particularly sensitive to measurement techniques, these plots are a good indication of the precision of the entire experiment.

Information about the influence of turbulent fluctuations on its surroundings can be found by examining the autocorrelation of the original

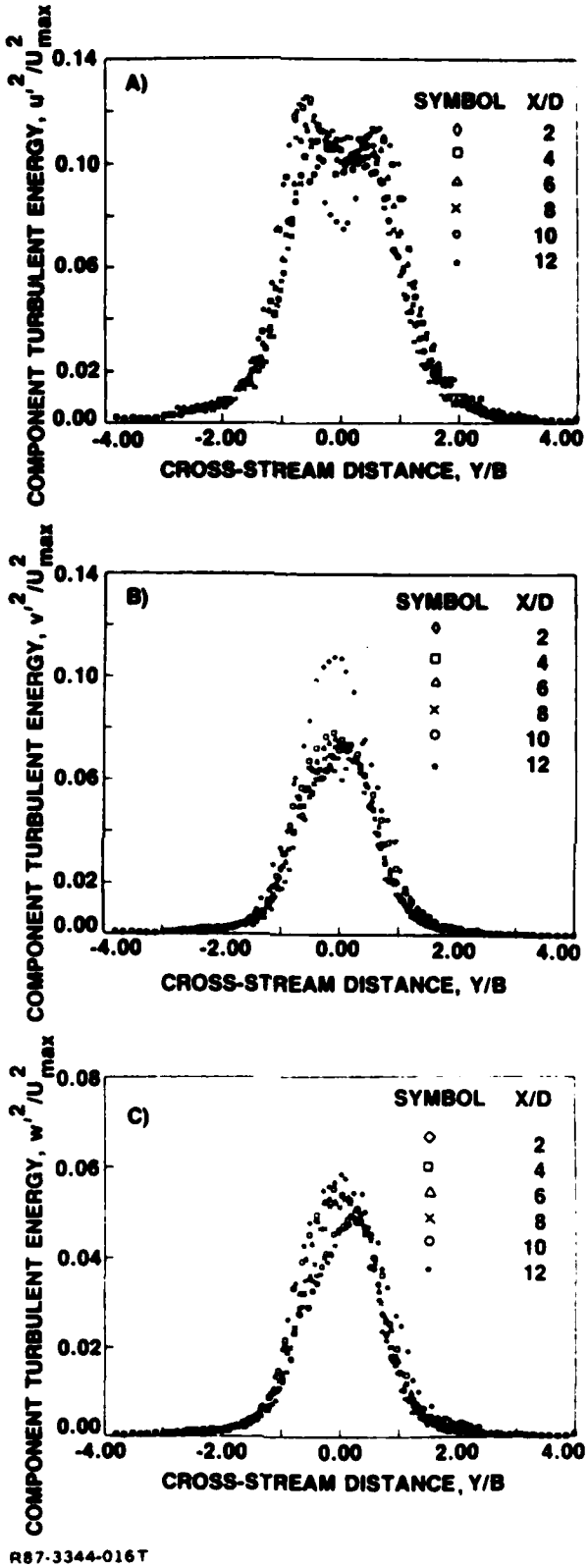


Fig. 21 Component Turbulence Energy at Six Heights

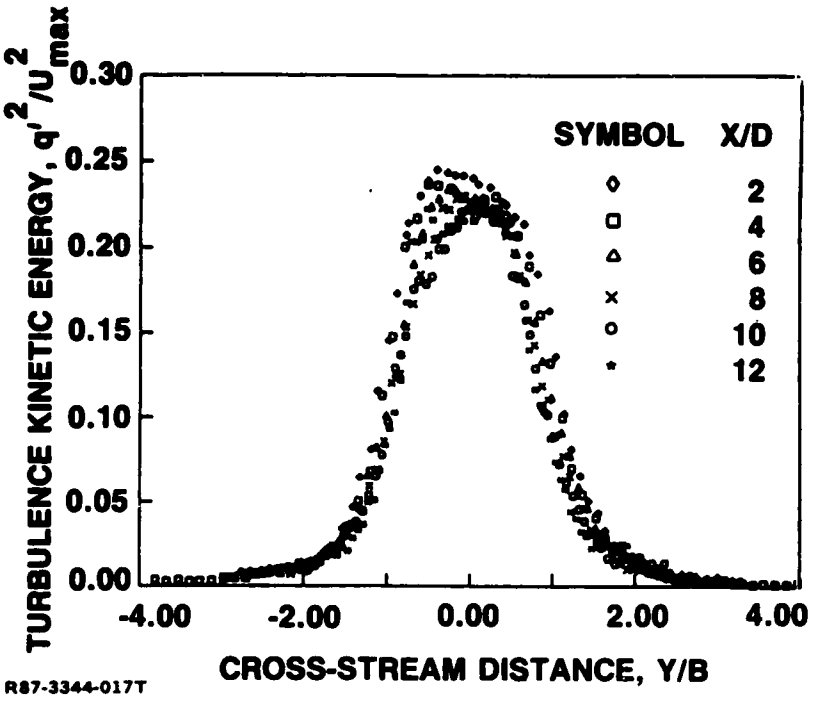


Fig. 22 Total Turbulence Kinetic Energy at Six Heights

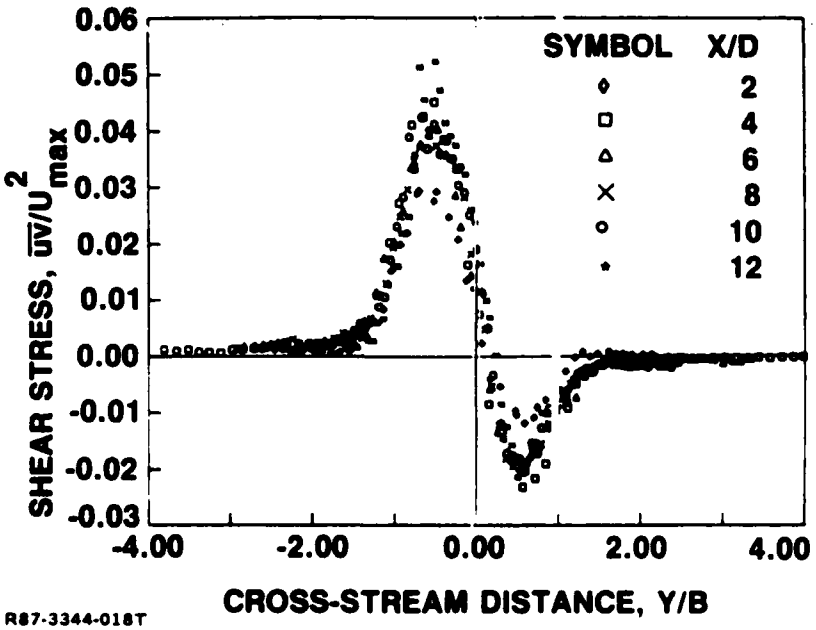


Fig. 23 Shear Stress Component at Six Heights

time series. The autocorrelation can be thought of as a measure of the physical extent of the influence of a fluctuation at a point. A measure of this quantity then gives an idea of the length of mixing involvement. This scale is called the integral length scale because it is defined as the integral under the autocorrelation curve. Since the autocorrelation is also the inverse Fourier transform of the power spectral density function, it does not give any additional information about the flow. It does, however, give another physical interpretation to the length scales identified in the spectral representation.

An additional length scale often used to describe turbulence is the Taylor microscale. While the scale really has no physical significance, the Taylor microscale is related to the overall energy dissipation. If one considers that all of the energy is dissipated by eddies of one size, those eddies would be the size of the Taylor microscale. It is always much smaller than the integral scale.

It is apparent from the three length scale profiles shown in Fig. 24 that the large scale eddies at the half width position are nearly as large as the upwash width itself. These integral scale lengths were obtained by integrating the area under the autocorrelation curve to the point of the first zero crossing. This length scale is representative of the size of the large scale motions (eddies) responsible for mixing. Through the center region, it is seen that these eddies are a significant percentage of the local mean velocity half width. The eddies are much larger than those found in a free jet flow, again by a factor of two!

The three turbulent microscale lengths are shown in Fig. 25. The microscale length representative of the energy dissipation length, was calculated in two different ways. It was directly calculated from the derivative of the time series and applying Taylors' hypothesis. This method suffers from the inherent noise increase by differentiation. In addition, due to the intermittency away from the centerline, the average values at a point are prejudged towards lower values. The second method computes the scale from the second derivative of the autocorrelation function at the origin. At the centerline, these two methods give good agreement. Figure 25 utilizes the second method. The values are nearly constant across the mixing layer as assumed in some mixing length turbulence models. The values are unusually

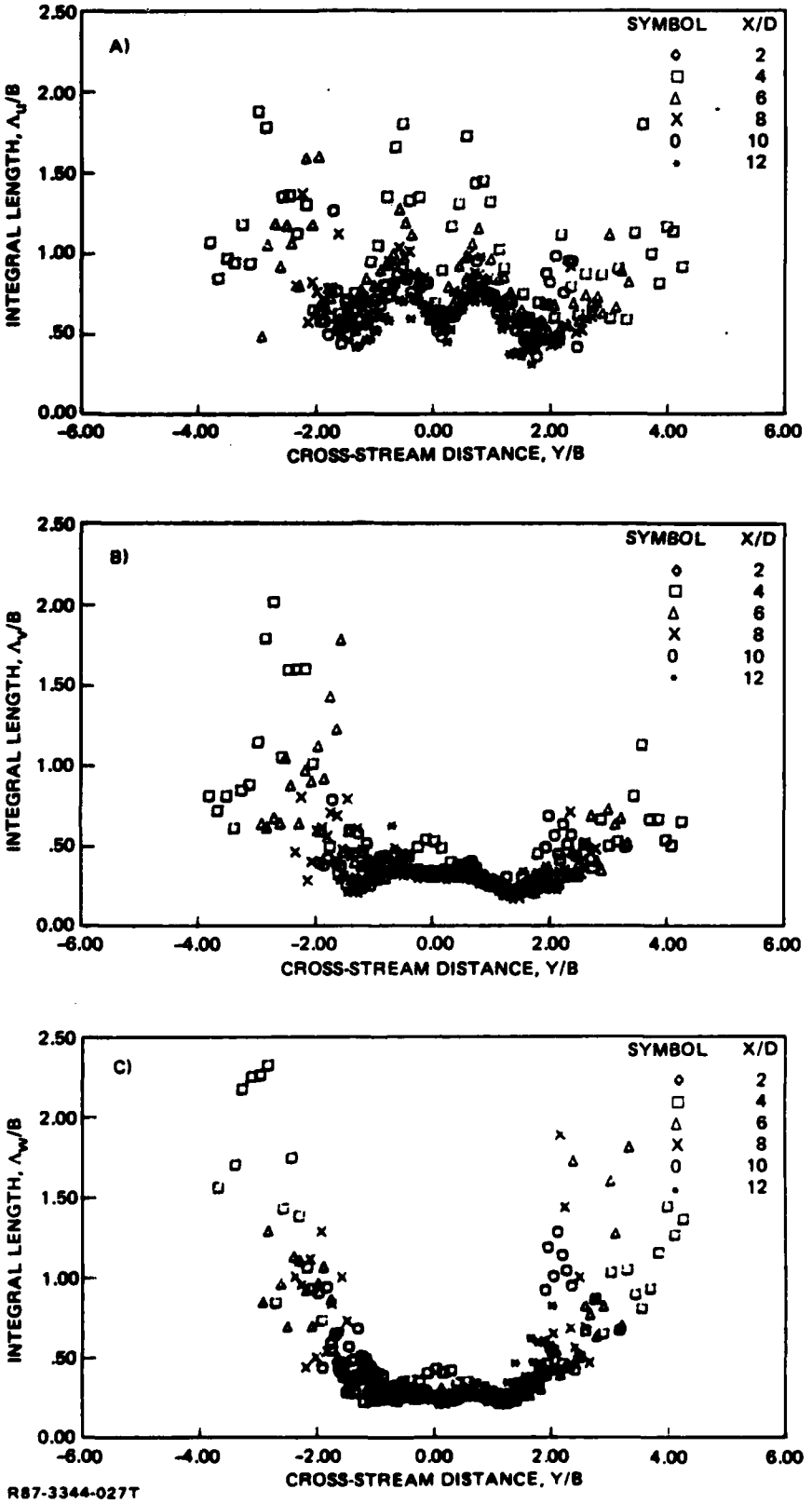


Fig. 24 Integral Scale Lengths

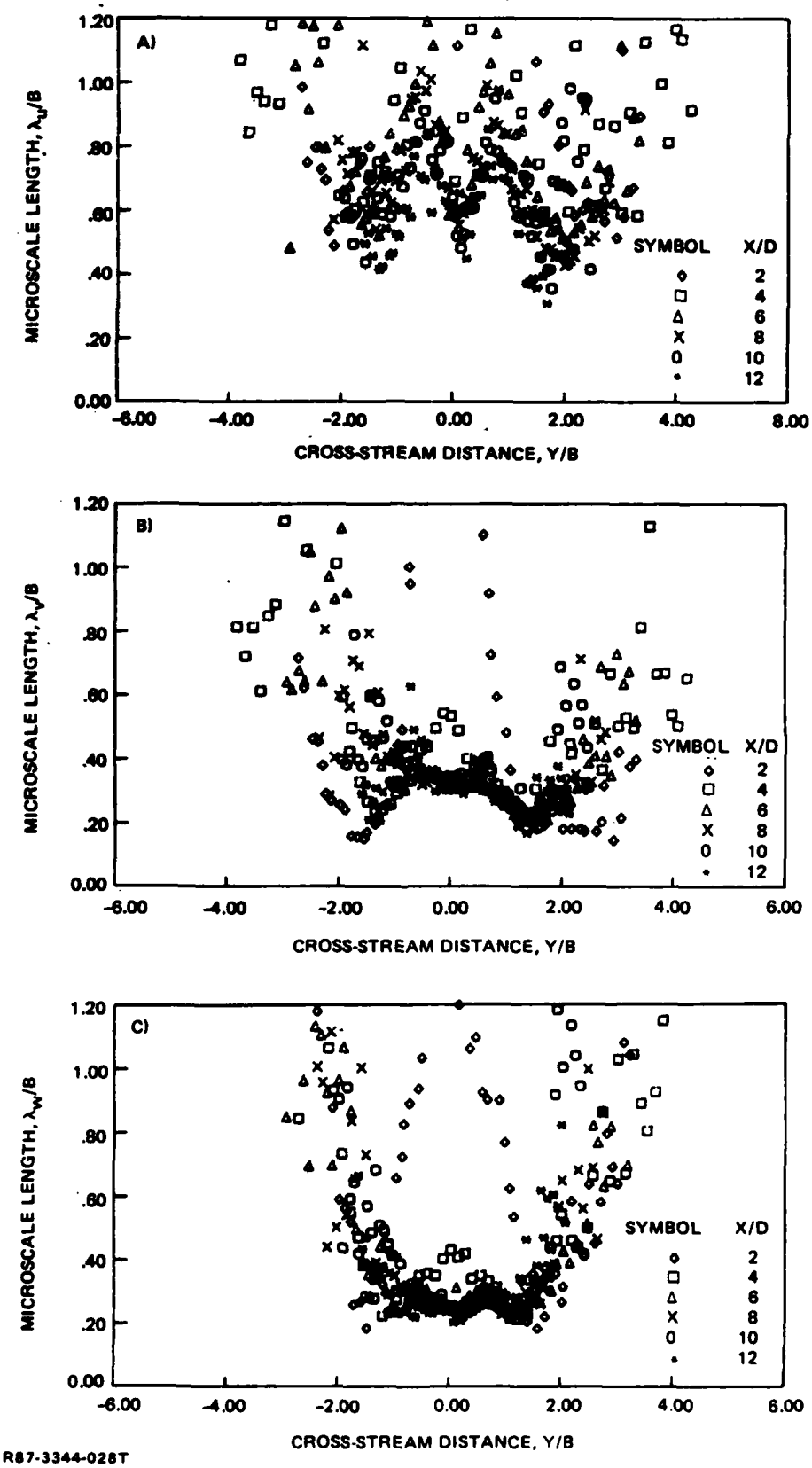


**Fig. 25 Taylor Microscale Lengths**

large, indicating greater than normal turbulence dissipation consistent with the increased mixing rate. Figure 25 shows nearly constant values of $\lambda/B$ in the upwash. Therefore, $\lambda$ must vary linearly at the same rate as B with X/D. Since $\lambda_u$ is approximately $\lambda_v$ the isotropic relation is valid in the self similar region of the upwash. The data should only be examined between $\lambda/D = \pm 2$. Outside of this value, the large intermittency creates a great deal of data scatter. The dissipation may be estimated from the isotropic relationship $\varepsilon = 30\nu\, u'^2\, U^2/\lambda_u^2$ .

The ratio of the two length scales is of the order of 2. This corresponds well to a condition of local isotropy. The large scatter of the "U" scale at the lower stations is due to the rapid momentum redistribution affecting the local correlation. Scatter for values $Y/B > 2$ or $< -2$ is an artificial effect due to the calculation method.

As in the two-dimensional upwash (Ref 13), the higher turbulent moments were also measured. The third moments are shown in Fig. 26, and the fourth moments in Fig. 27. Functions of u' are even (symmetric with respect to the centerline) and v' and w' are odd (asymmetric). Correlations of v and w vanish at the centerline and all functions attain a maximum around the half width, and then fall to zero at the outer edge. The variation across the centerline (slope) seems to be nearly linear. The symmetry of the even higher moments is very obvious. These are the moments that appear in the turbulent kinetic energy equation. The departure of these moments from Guassian contain the unique aspects of turbulences that must be considered in any model. Since these data are normalized as before, the important differences between these data and free jet data are hidden in the normalizing constants.

## 2.5 UPWASH MEASUREMENTS - OFF CENTERLINE

Figure 10 shows the positions used for off centerline measurements. Data taken at these positions were obtained using the short version of the data acquisition program. Only means, turbulence energy and one Reynolds stress component were obtained for each orientation of the X-probe. Two orientations at each position were used. The results are similar to those already presented in the centerline plane connecting the source jets. Measurements were made through the upwash on four planes parallel to the centerline plane. These planes were at positions 2D, 4D, 6D and -2D with respect to the centerline plane. All the statistics were computed as before.

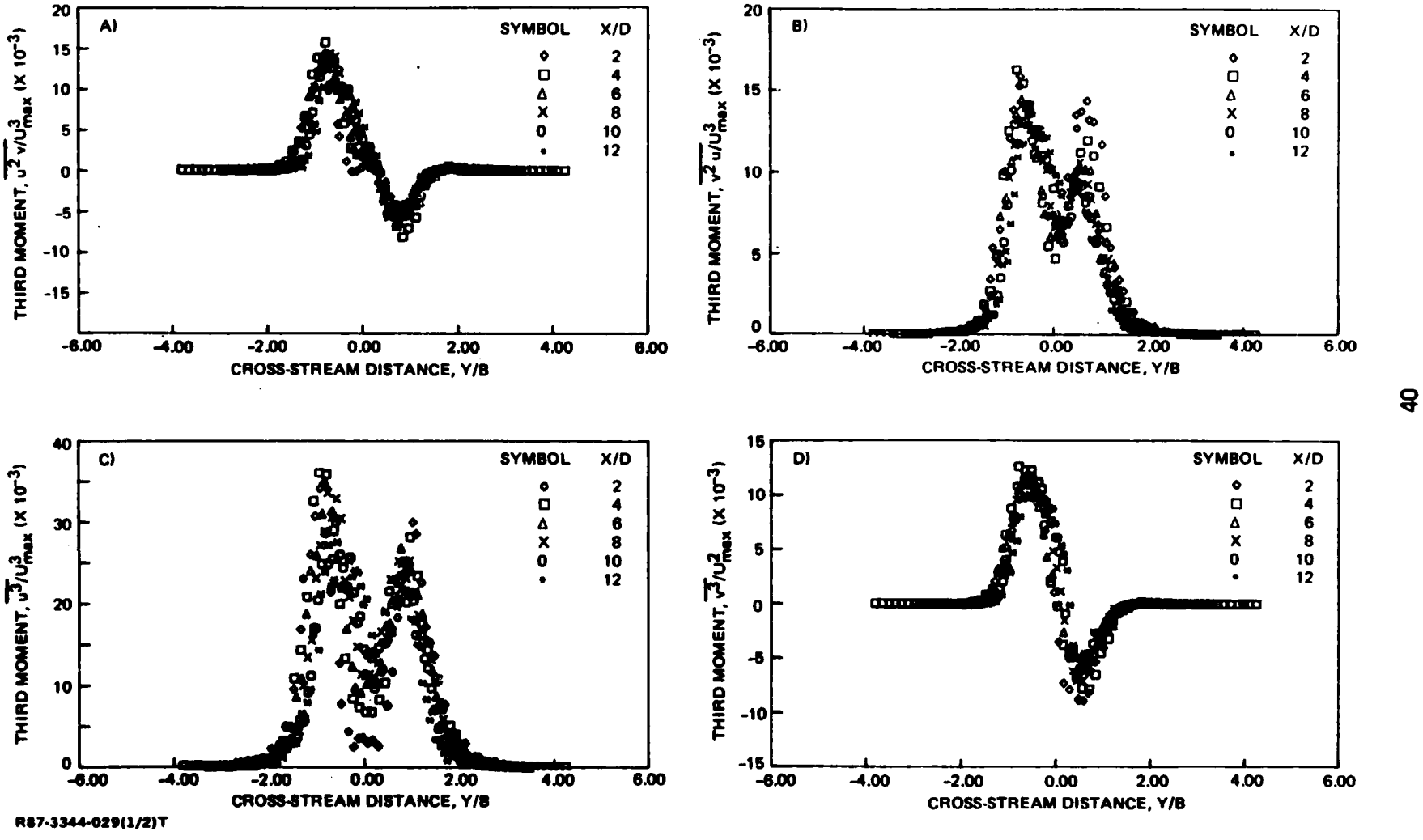


R87-3344-029(1/2)T

Fig. 26 Third Moments at Six Heights (Sheet 1 of 2)

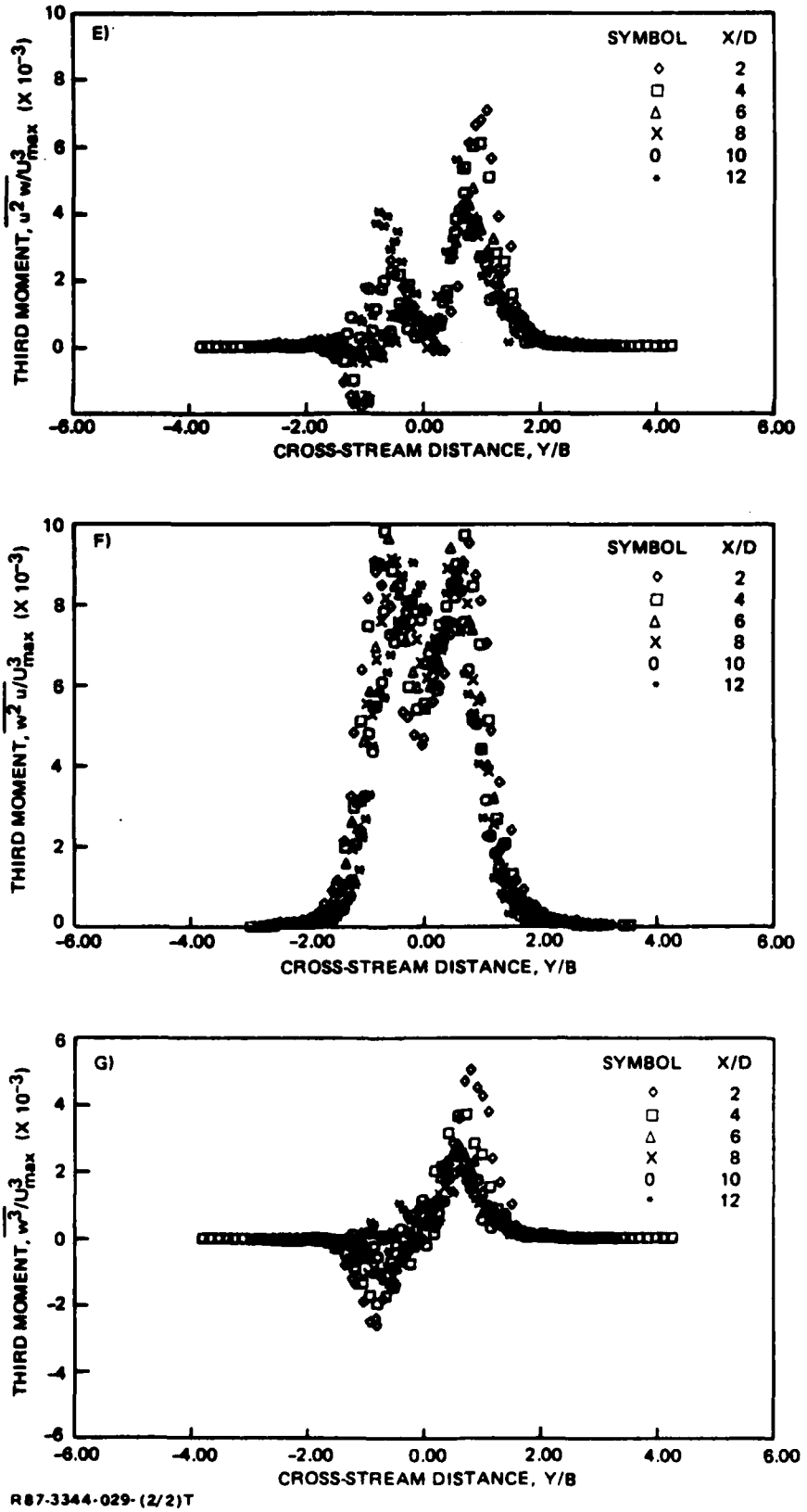


Fig. 26 Third Moments at Six Heights (Sheet 2 of 2)

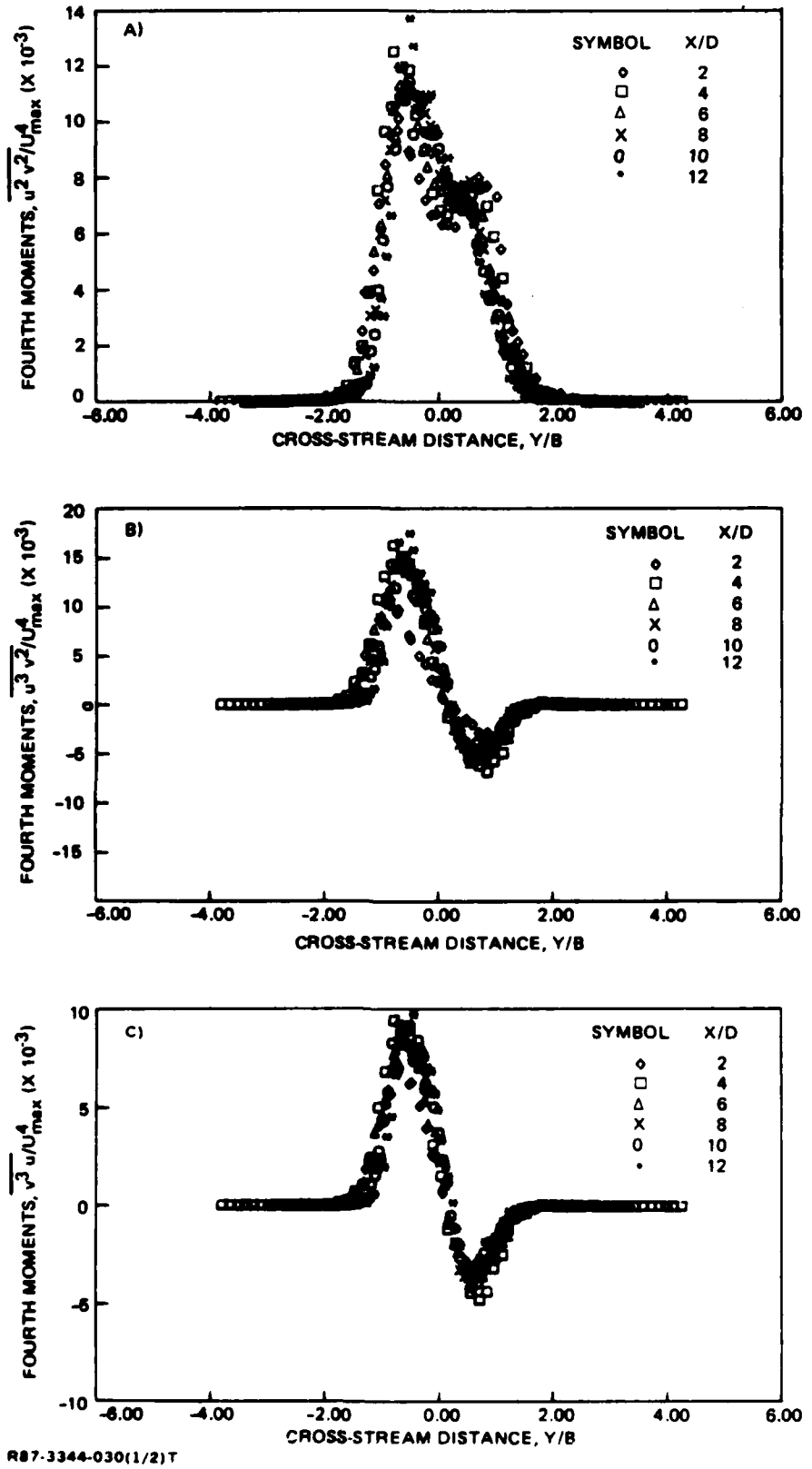


Fig. 27 Fourth Moments at Six Heights (Sheet 1 of 2)

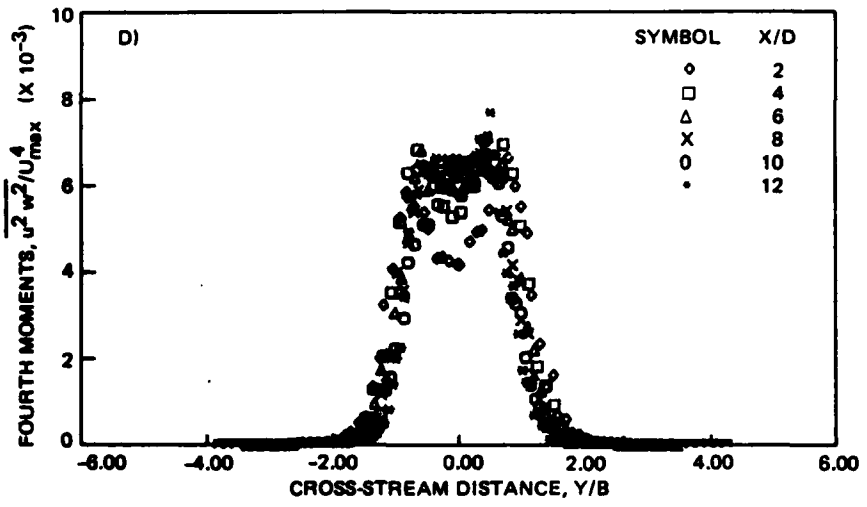


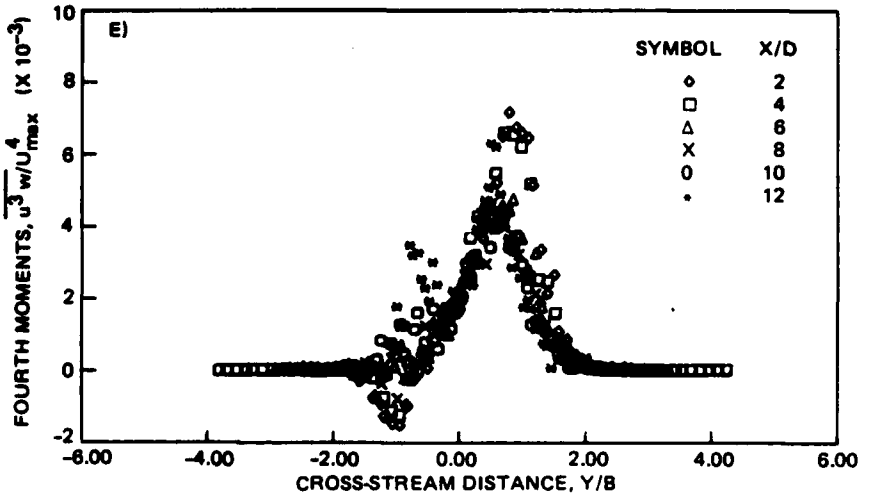


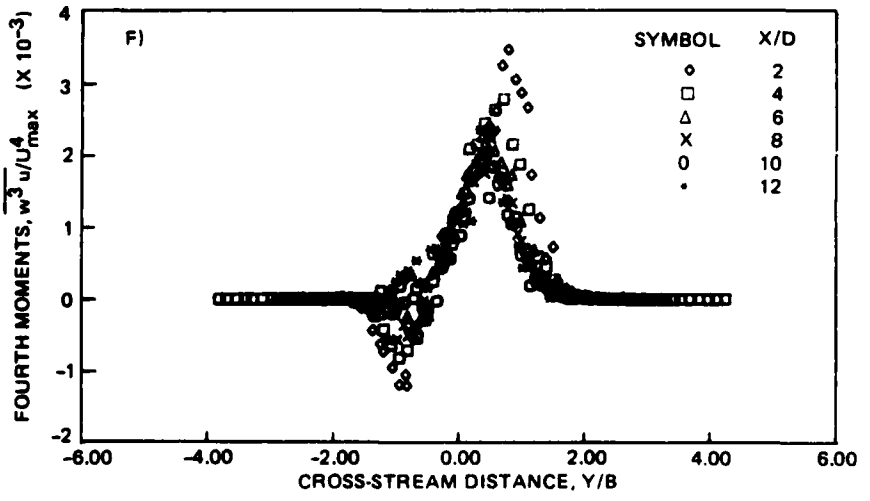


R87-3344-030(2/2)T

*Fig. 27 Fourth Moments at Six Heights (Sheet 2 of 2)*

Figure 28 shows the mean velocity normalized by the local maximum velocity at four heights (six on the centerline) in each of the five parallel planes. The centerline data at heights 10D and 12D show some distortion due the presence of the probe supports.

The half velocity growth rate for each set of data is shown in Fig. 29A. The slightly slower growth rate which is seen farther away from the centerline occurs because the flow has traveled a farther distance from the origin by the time it gets to each height and, therefore, has had longer to decay. This can be seen in Fig. 1. At ± 2D the effect is small. However, for Z/D = 6, the measurement station is as much as 1.8D farther downstream from the virtual origin than the equivalent position in the centerline. The growth rate decreases from a maximum of 0.25 at the centerline to 0.20 six characteristic dimensions outboard.

Figure 29B shows the linear decay rates. The lower maximums at any height away from the centerline are very apparent. While the values are lower, the rates as shown by the slope of the curves are almost constant. Important empirical parameters are summarized in the following table.

TABLE 1. SUMMARY OF PARAMETERS OFF THE CENTERLINE

| Z/D | Growth Rate | Decay Rate | Mass Coefficient | Entrainment Rate | Momentum Coefficient |
|---|---|---|---|---|---|
| 0 | 0.252 | 0.638 | 0.177 | 0.269 | 1.01 |
| 2 | 0.230 | 0.609 | 0.169 | 0.245 | 1.01 |
| 4 | 0.222 | 0.605 | 0.165 | 0.236 | 0.99 |
| 6 | 0.195 | 0.561 | 0.156 | 0.208 | 1.01 |
| -2 | 0.250 | 0.654 | 0.172 | 0.266 | 0.95 |

The normalized total kinetic energy is shown in Fig. 30 and turbulent components are shown in Fig. 31 through 33. Finally, the Reynolds stress are shown in Fig. 34. These values are included primarily for completeness. The form and magnitude of these data are very similar to those presented for the centerline. The main purpose of these data is to show that the upwash fan is well behaved even far from the centerline plane. Note that the Reynolds

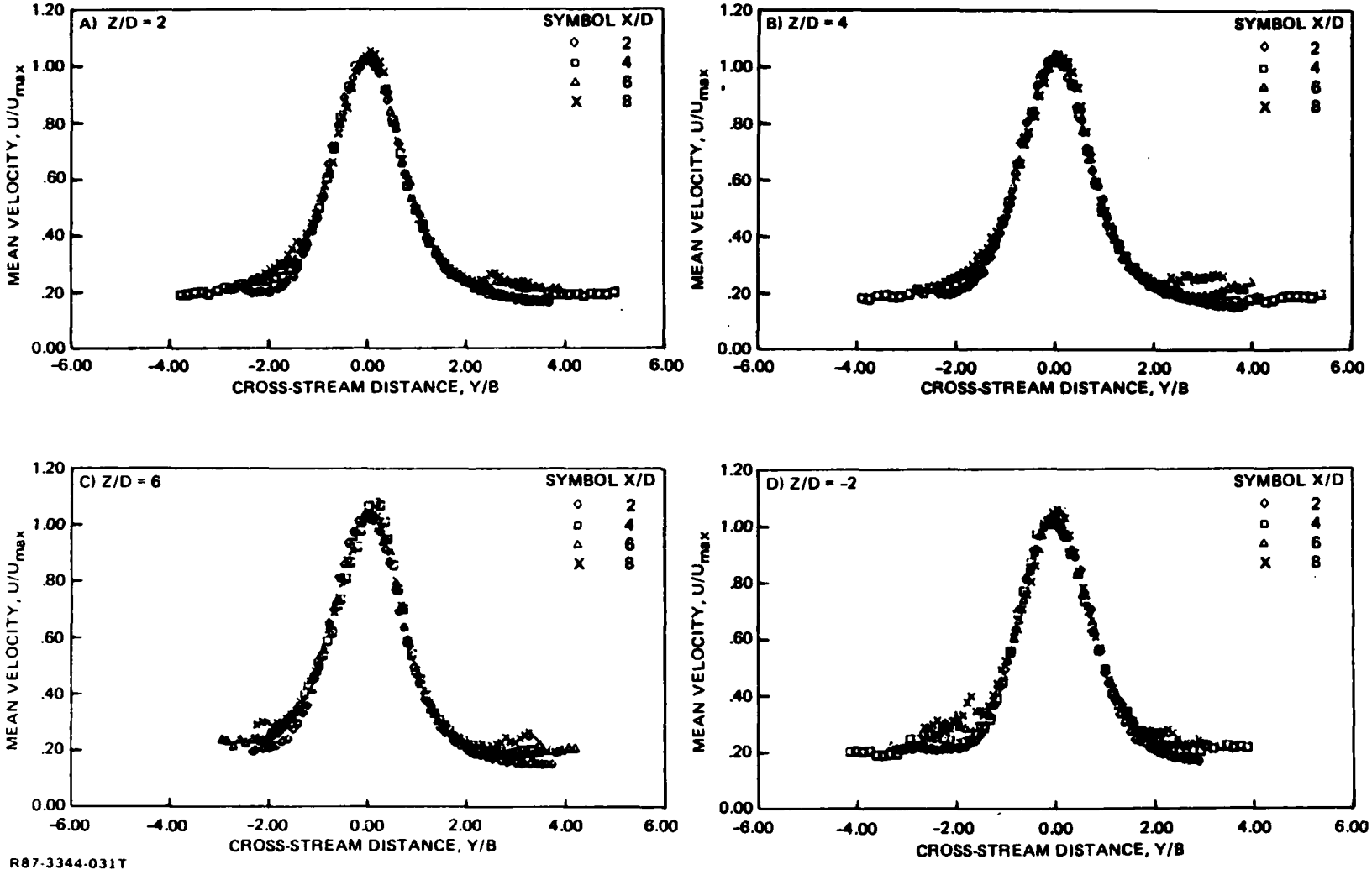


Fig. 28 Mean Velocity Profiles Off Centerline in Similarity Form

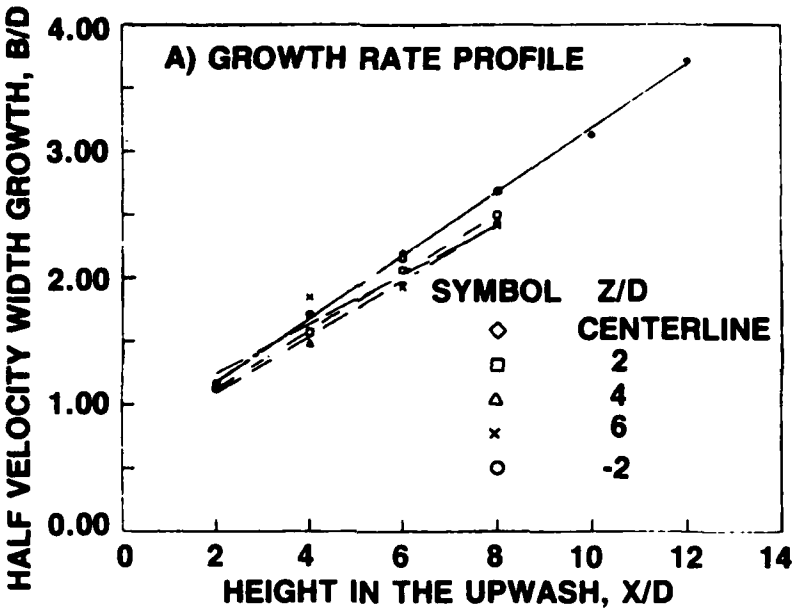


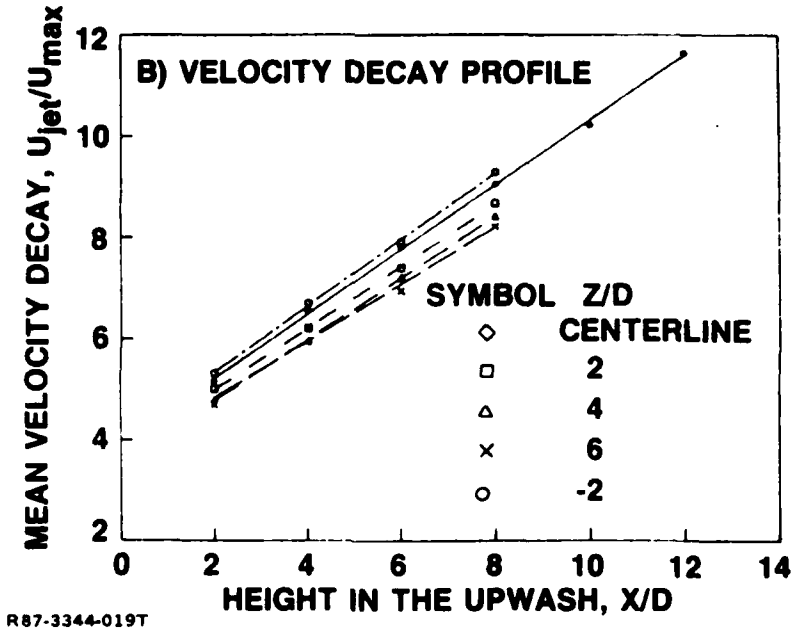


Fig. 29 Radial Upwash Characteristics Off the Centerline

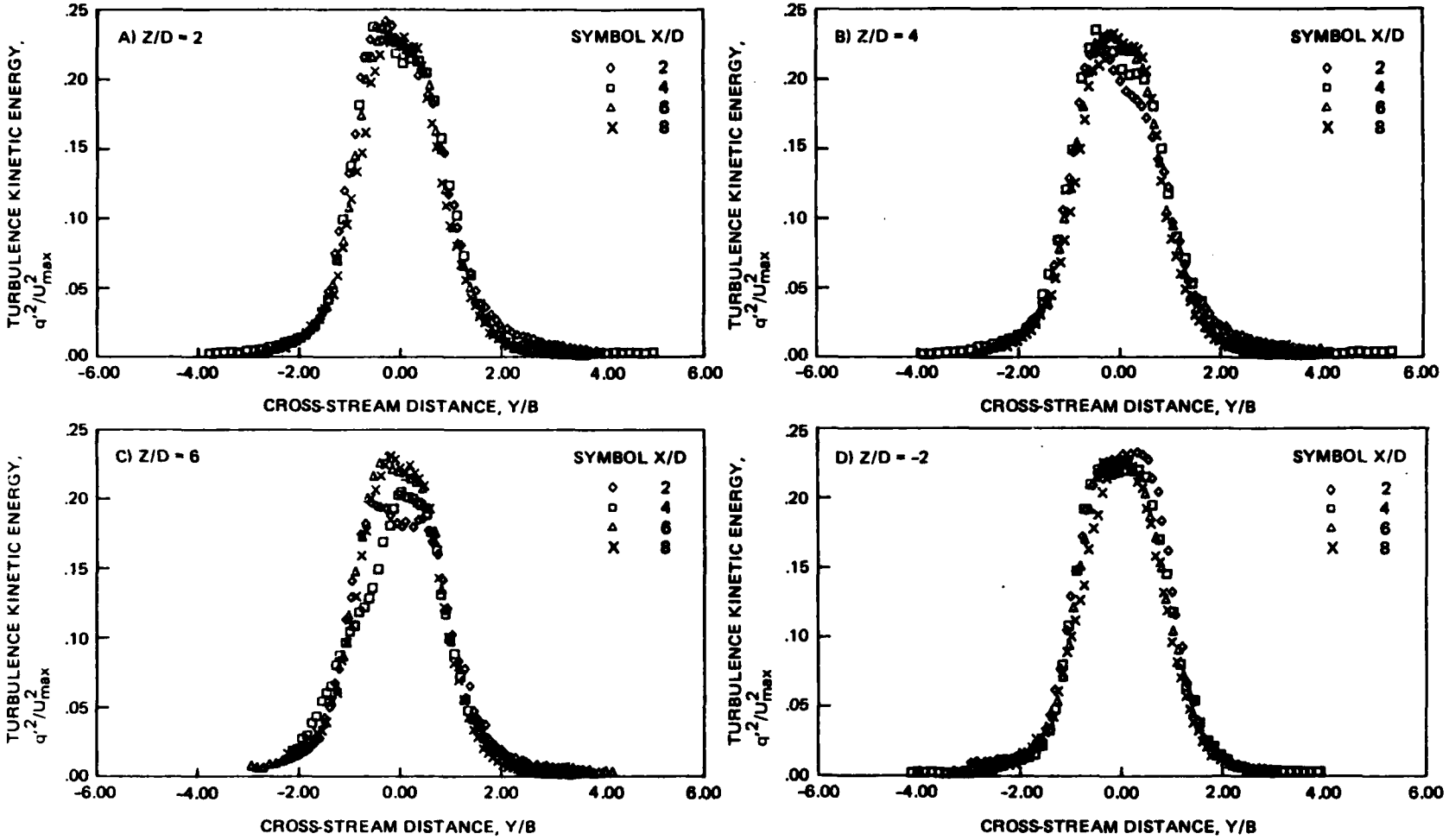


Fig. 30 Total Turbulence Kinetic Energy Off the Centerline

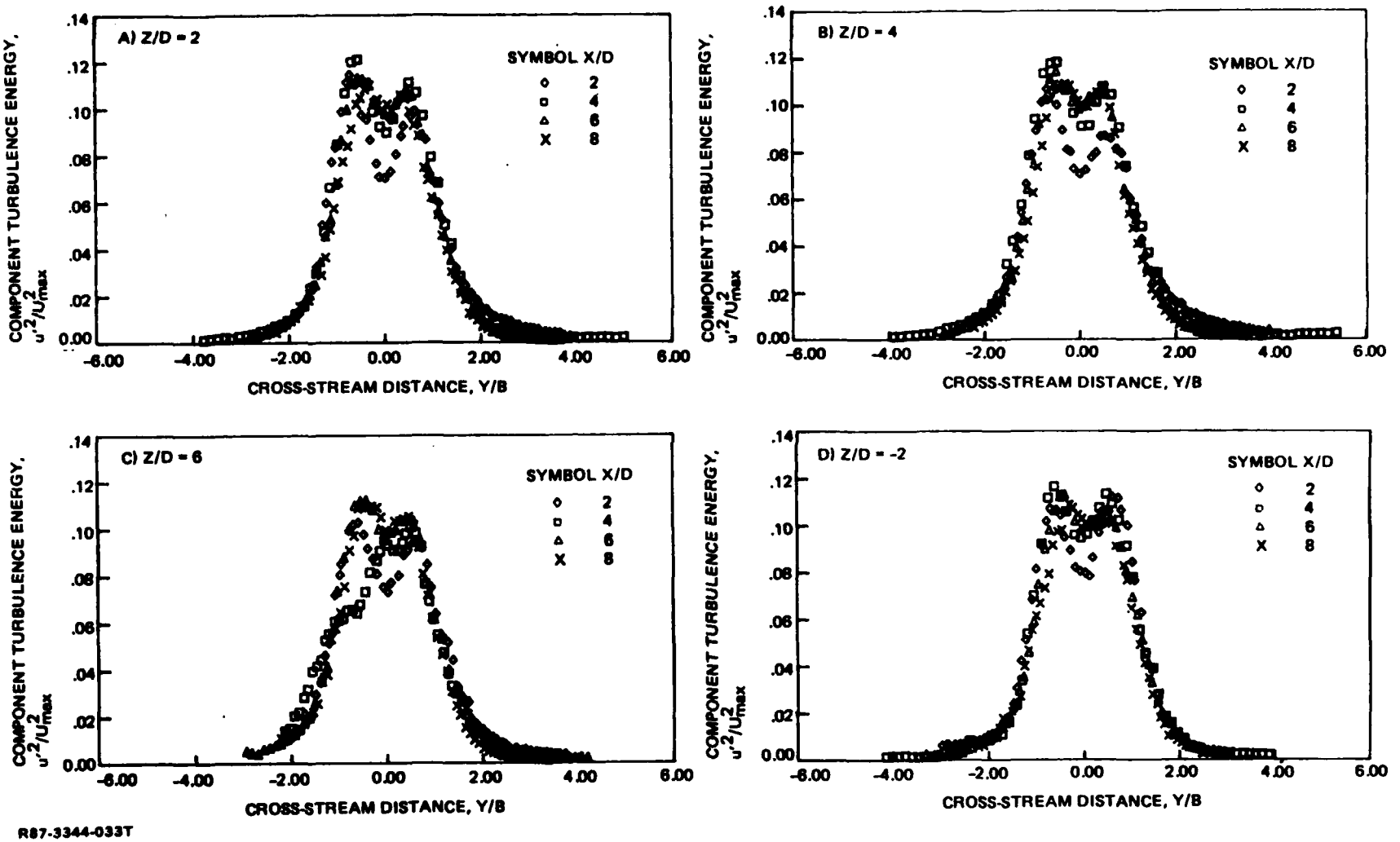


Fig. 31 Component Turbulence Energy in the Mean Flow Direction Off the Centerline

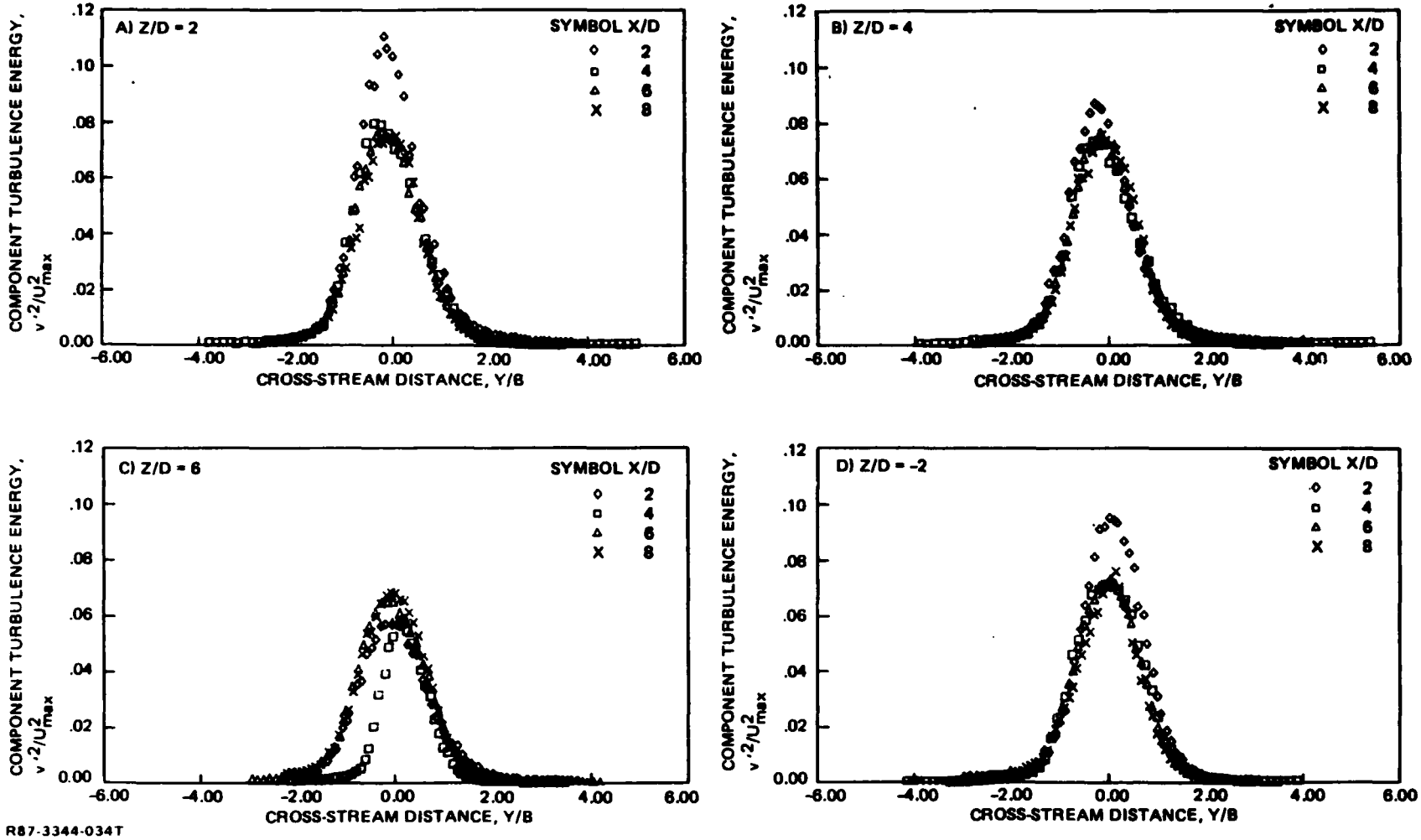


Fig. 32 Component Turbulence Energy in the Cross-flow Direction Off the Centerline

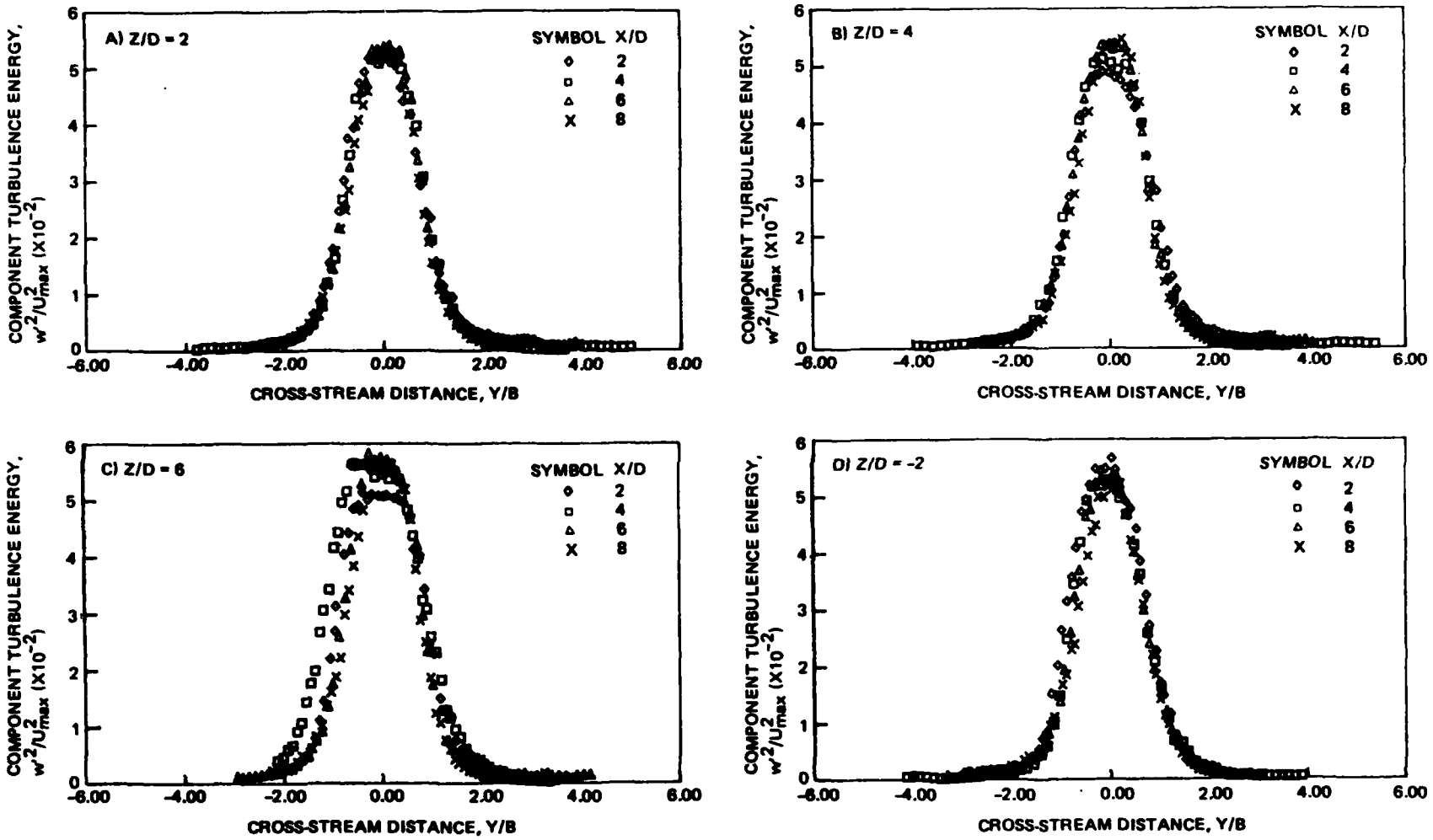


R87-3344-035T

**Fig. 33 Component Turbulence Energy in the Third Normal Direction Off the Centerline**

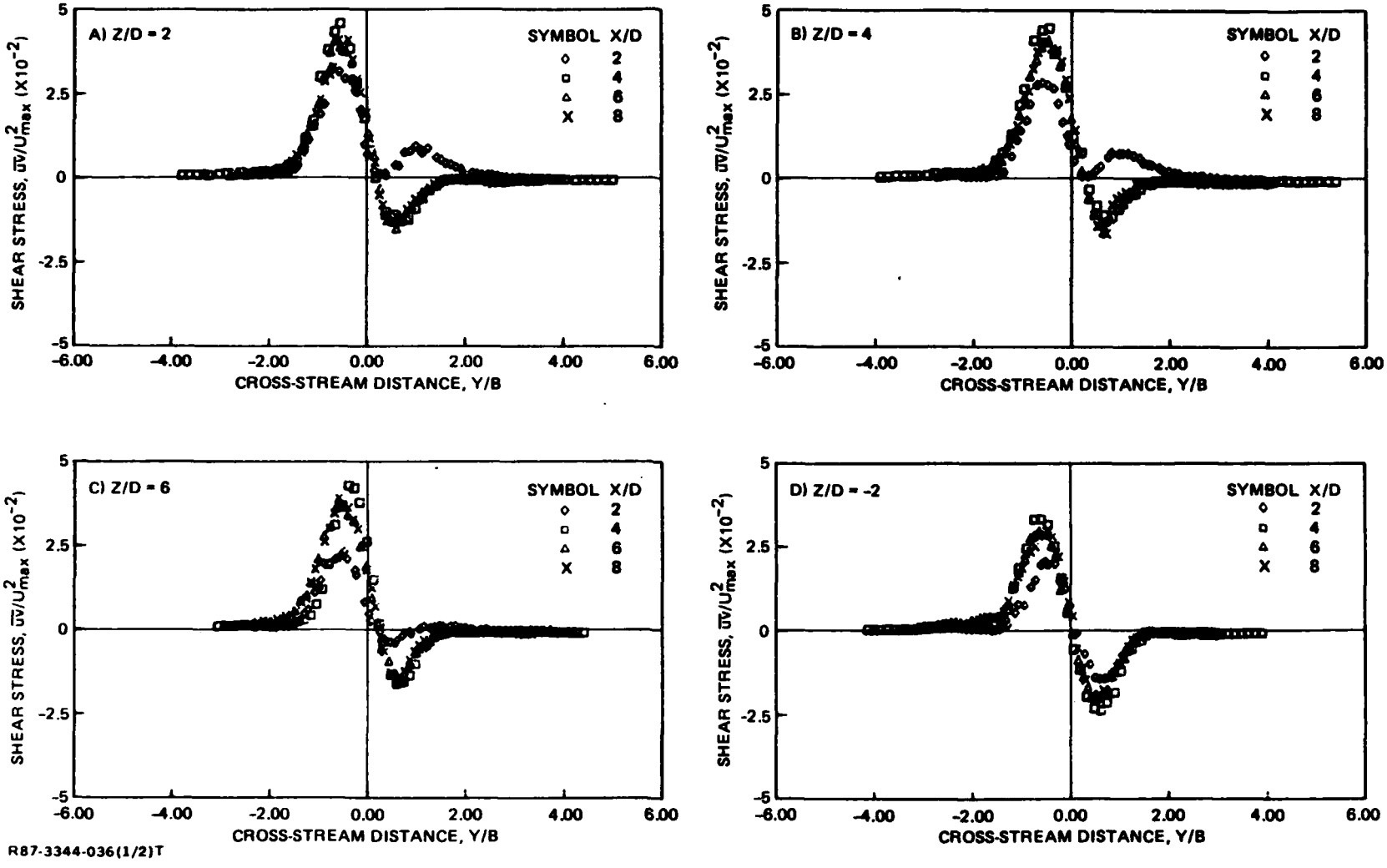


R87-3344-036(1/2)T

**Fig. 34 Shear Stress Component Off the Centerline (Sheet 1 of 2)**

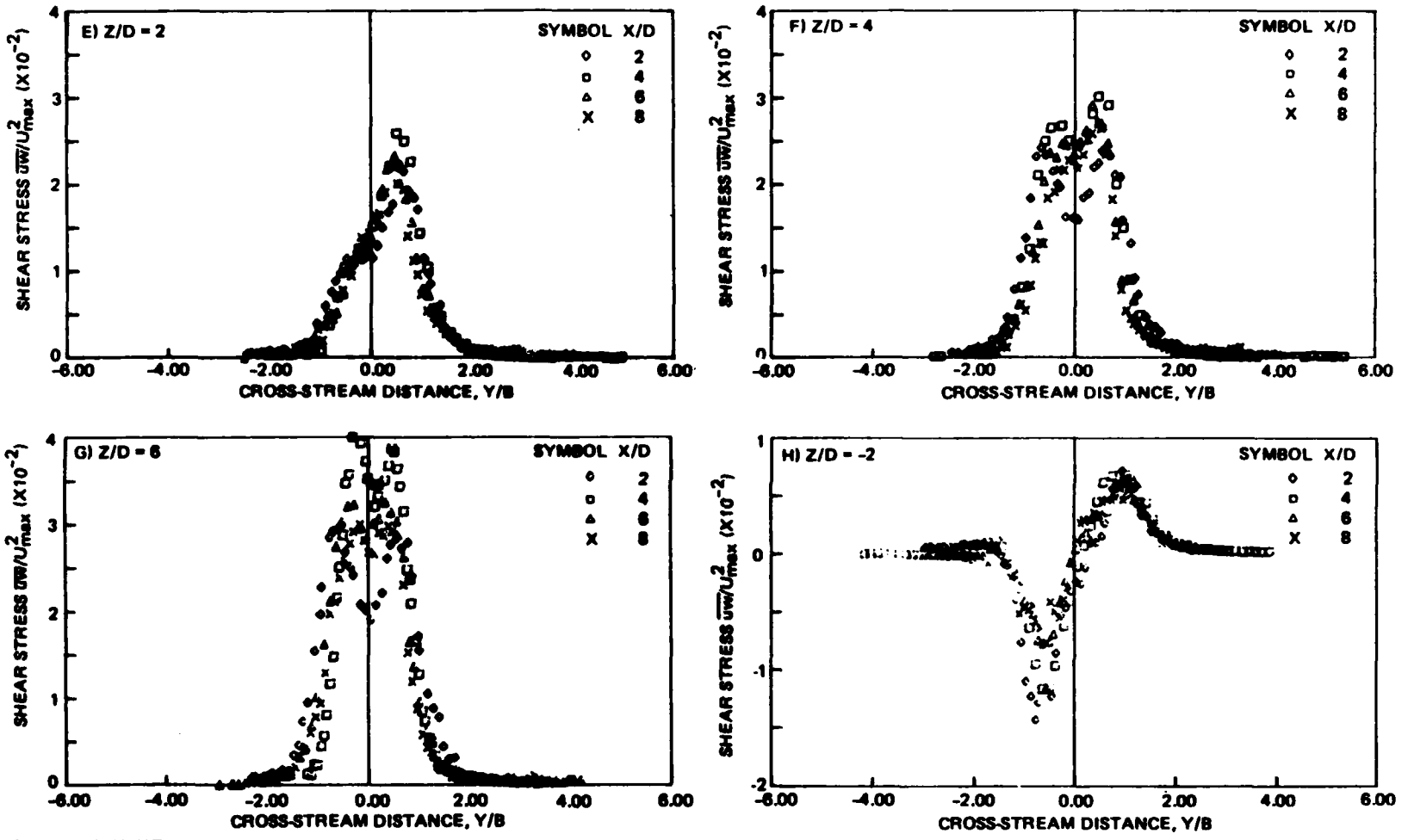


R87-3344-036(2/2)T

**Fig. 34 Shear Stress Component Off the Centerline (Sheet 2 of 2)**

stress effect described earlier persists across the layer. At Z/D = -2, (Fig. 34d) the magnitudes of the peaks are nearly equal. The slight skewness of the upwash sheet appears in the off center form of uw at Z/D = 2 (Fig. 34e), when compared to a more expected form at Z/D = -2 (Fig. 34h).

Because measurements were made using an X-probe, mean velocities V and W were also obtained with no directional ambiguity. While the two source radial jets were set in every way similar, a slight preference of the upwash sheet to bend to one side was seen in the V mean data. This is the direction connecting the source jets. The magnitude of this velocity component decreased rapidly with height above the ground. The maximum at the lowest station was less than 15% of the local mean velocity in the X or upwash direction. This represents a slight variation in flow angle from vertical by less than 10°. The two-dimensional wall jet upwash flows did not have this type of behavior. By slightly rearranging the orientation of the observation plane for alignment with the centerline mean velocity vector, the remaining V velocities are as expected. These are shown in Fig. 35. At X/D = 2, the measurement station is still in the turning region. This can be seen quite obviously by the reversal of the V component at the lower stations to the higher ones. Positive values represent a flow to the left. Between Y/D = ±1, the flow is well behaved. Note the maximum value of the cross-stream velocity is less than 5%.

The W velocity is in the direction perpendicular to the plane connecting the source radial wall jets. Referring to the symmetry plane shown in Fig. 1, this is the component of mean velocity away from the centerline plane. These data are shown in Fig. 36. As expected, in the symmetry plane, the component farthest away from the centerline plane is the greatest. Away from the symmetry plane, entrainment and the lesser influence of the collision zone mean that the flow is more vertical.

The flow in the symmetry plane was measured separately with the X-probe traversed along the plane. From these data, it is possible to compute the velocity vector in the plane perpendicular to the line connecting the source jets. The theory derived from a simple conservation criterion requires that all of these vectors are straight and emanate from the same virtual origin. The measured values with the theoretical prediction for the symmetry are shown in Fig. 37. To the positive Z-side, the agreement is very good. On the

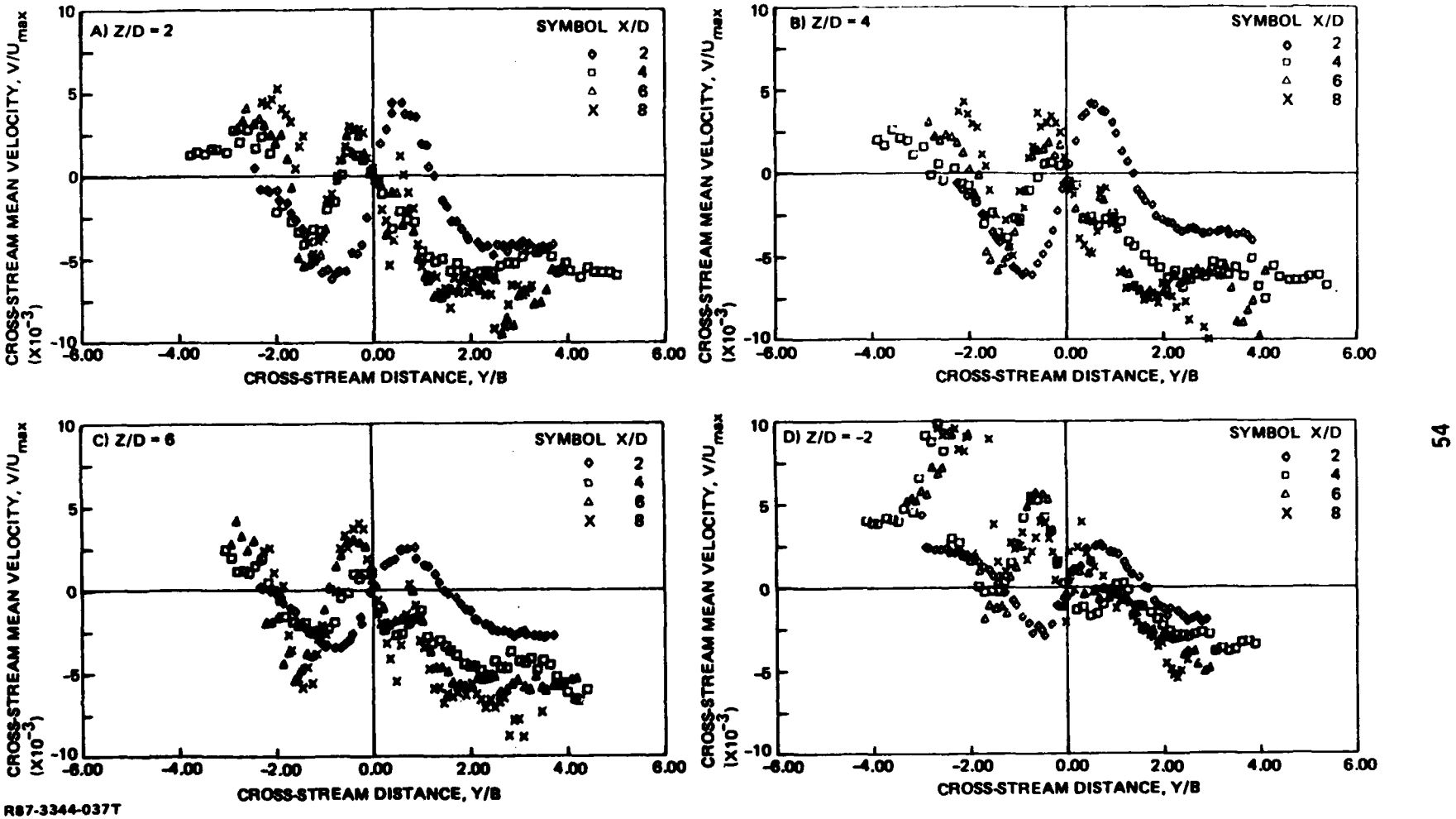


Fig. 35 Cross-stream Mean Velocity in a Rotated Frame Off the Centerline

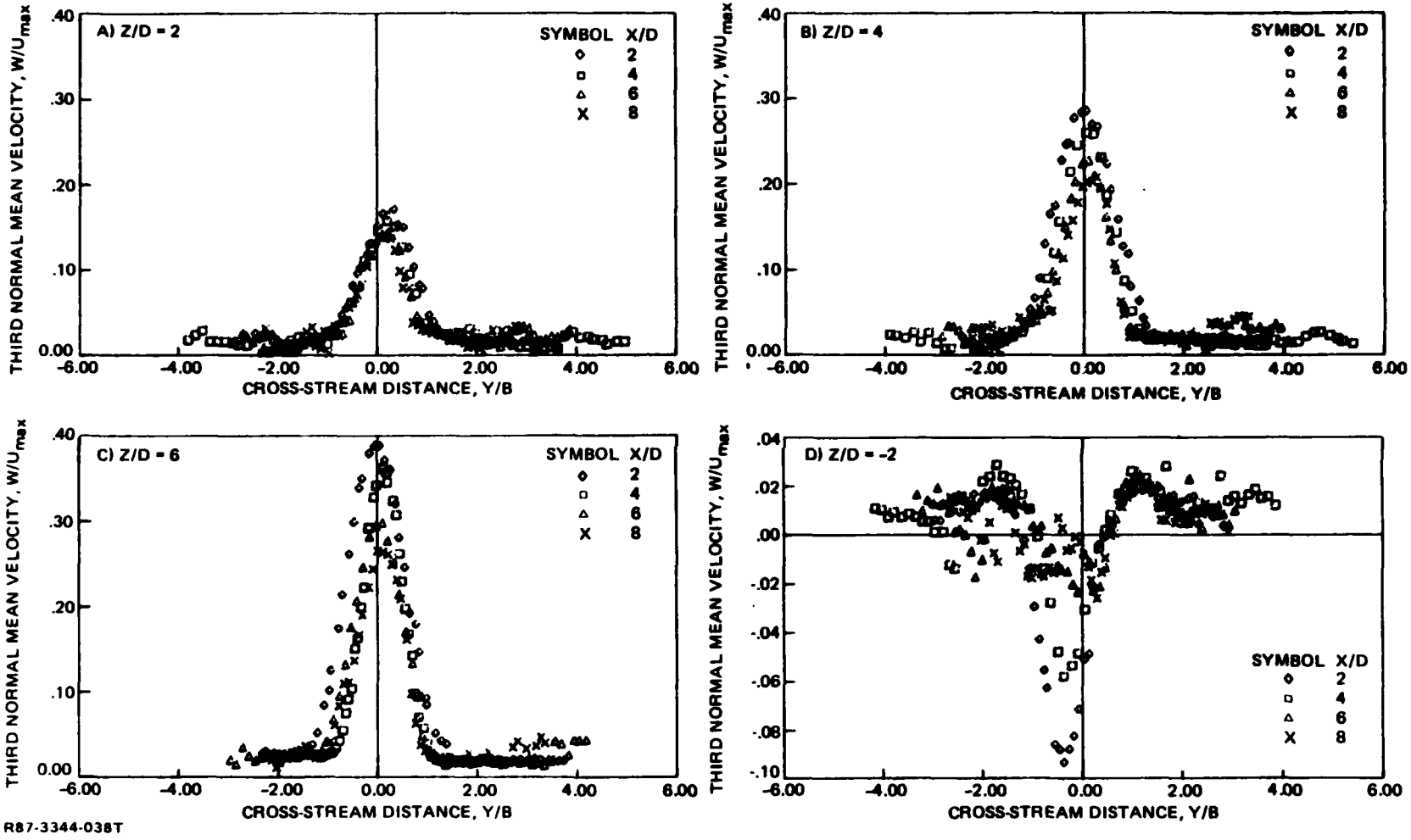


Fig. 36 Third Normal Mean Velocity Component Off the Centerline

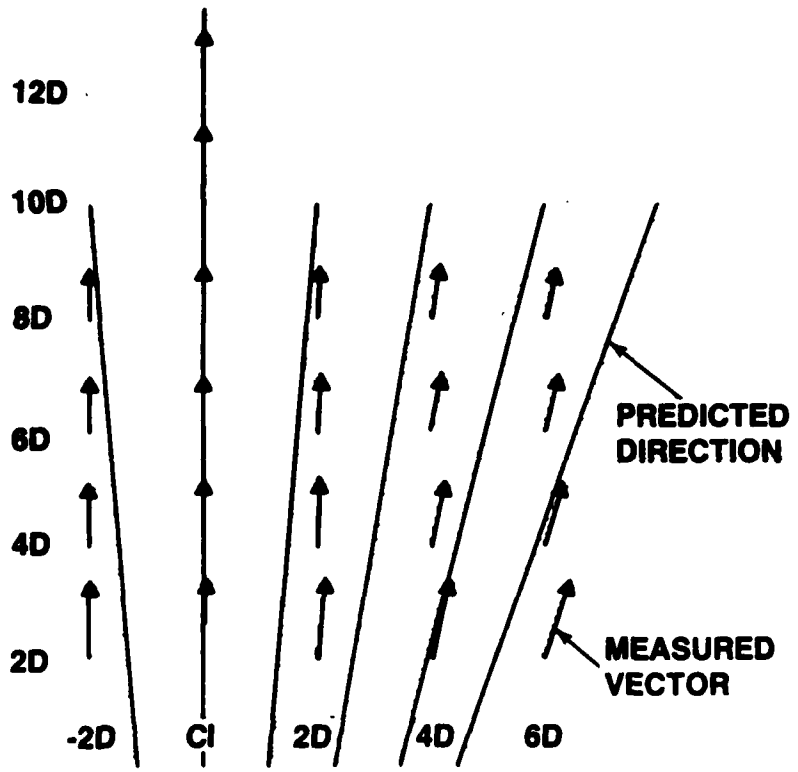


R87-3344-020T

Fig. 37 Measured and Predicted Velocity Vectors in the Symmetry Plane

negative side, the vectors seem to point more closely to the vertical. Planes parallel to the symmetry plane are shown in Fig. 38. The vectors turn more toward the vertical as you go away from the symmetry plane. This is reasonable since this flow is more influenced by entrainment and less by the direct collision with the opposing wall jet. The reason that the negative side vectors are different from the positive is a small wrinkle in the upwash fan. Throughout the initial stages of setting up this experiment, it was continuously re-emphasized that even a small variation in the wall jet profiles along the collision line would result in a slanting or wrinkling of the upwash fan.

## 2.6 GROUND PLANE PRESSURES

A rotating plate in the center of the ground instrumentation plate allowed us to measure ground pressures. The circular plate had 8 pressure taps located at the centerline,1,2,4,6,8,10,and 12 cm in a log spiral arrangement as shown in Fig. 39A. The taps were connected to a scanivalve. The plate was rotated to a position, the scanivalve activated with enough time delay for the transconductance transducer to acquire the next pressure. The plate was moved in 15° increments to 25 locations. The first and last being the same to test for drift. This gives 7 x 24 = 168 unique pressure points over a 24 cm diameter circle from a point centered between the source jets.

Contour plots for various pressure ratios are shown in Fig. 39. These are the only tests reported here for unequal jet strengths. The contour lines shown in each of these figures are for values of static pressure equal to 0.0, 0.2, 0.4, 0.6, and 0.8 of the centerline pressure for an equal jet collision. Values of 0.0 are possible because there are places where the pressure actually goes negative with respect to ambient far away from the collision zone. All contours should close eventually but sometimes outside of the tap hole range shown in Fig. 39A.

In the equal radial wall jet case shown in Fig. 39B, the centerline pressure reached a value that exceeded the value corresponding to the complete conversion of a single radial wall jet mean velocity to a total pressure by 47.5%. That is, by simply bringing the wall jet to an isotropic stop does not account for the large increase in ground plane static pressure. Most of this static pressure seems to be recovered by accelerating the flow vertically. This pressure rise is primarily responsible for the momentum redistribution.

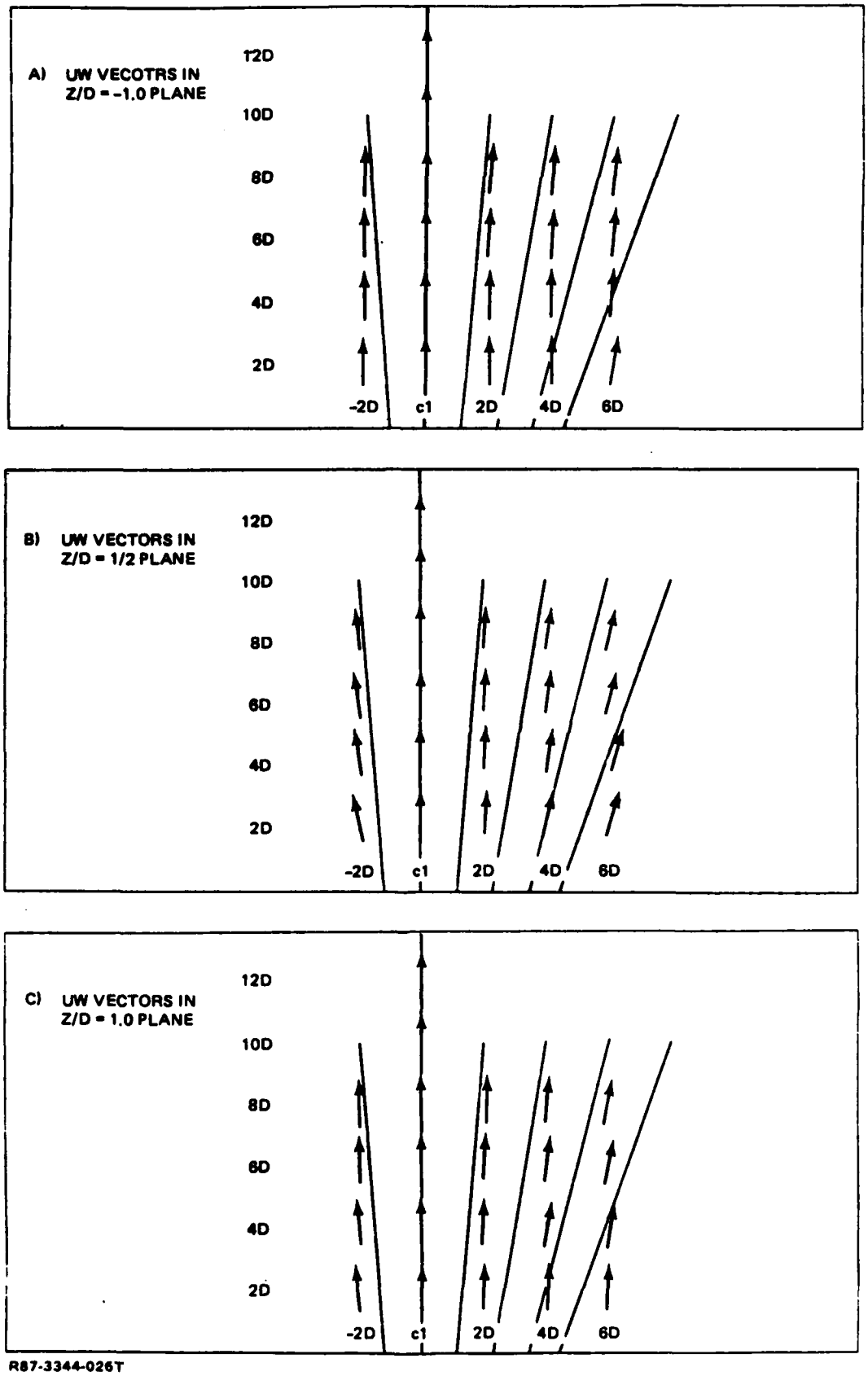


R87-3344-026T

**Fig. 38 Measured and Predicted Velocity Vectors in Planes Parallel to the Symmetry Plane**

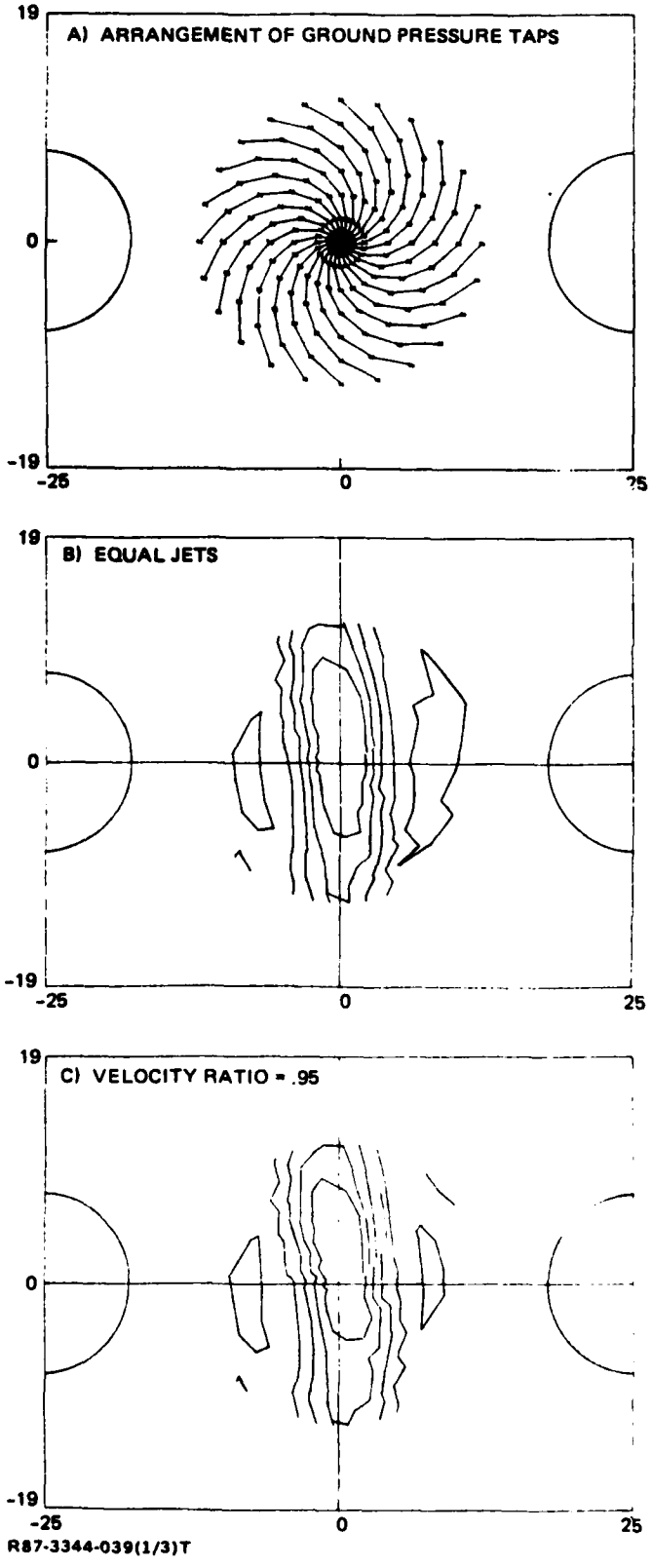


**Fig. 39** *Ground Plane Pressure Contours for Various Source Jet Velocity Ratios (Sheet 1 of 3)*

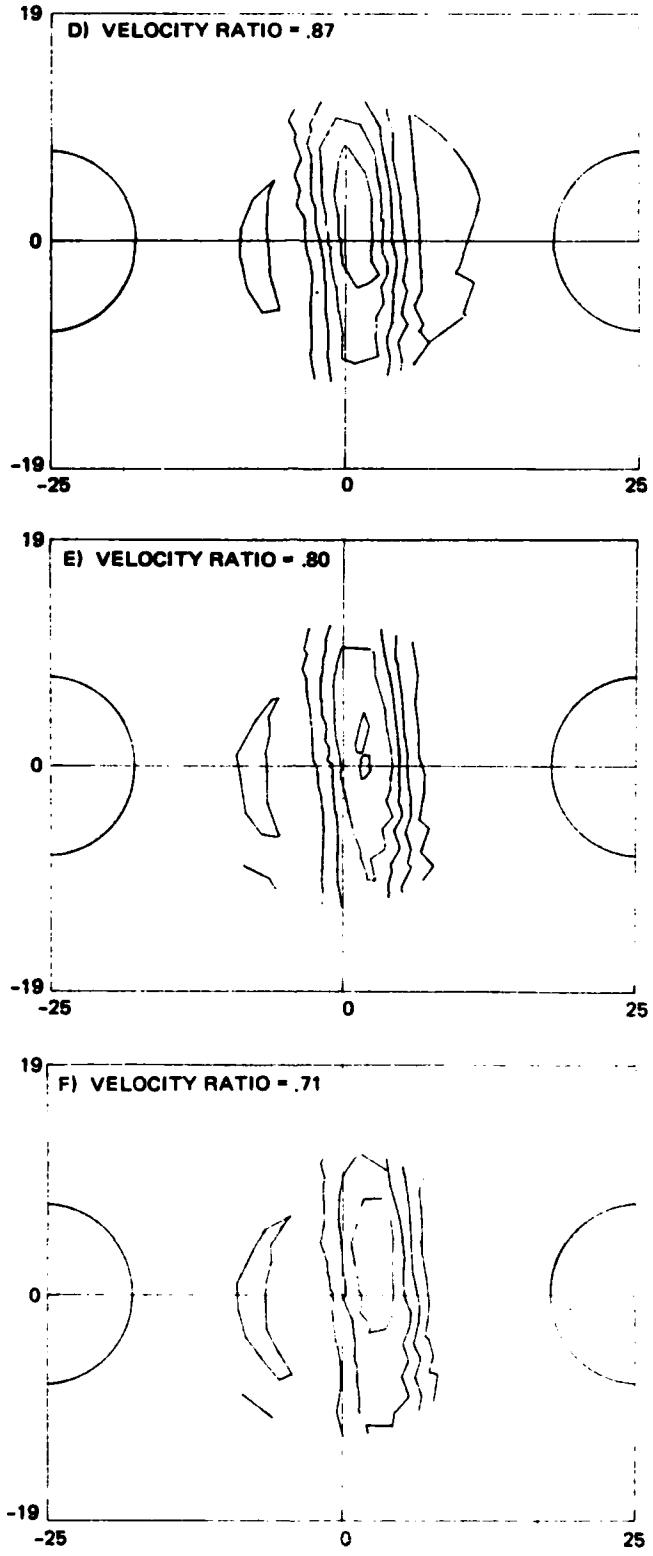


R87-3344-039(2/3)T

**Fig. 39 Ground Plane Pressure Contours for Various Source Jet Velocity Ratios (Sheet 2 of 3)**

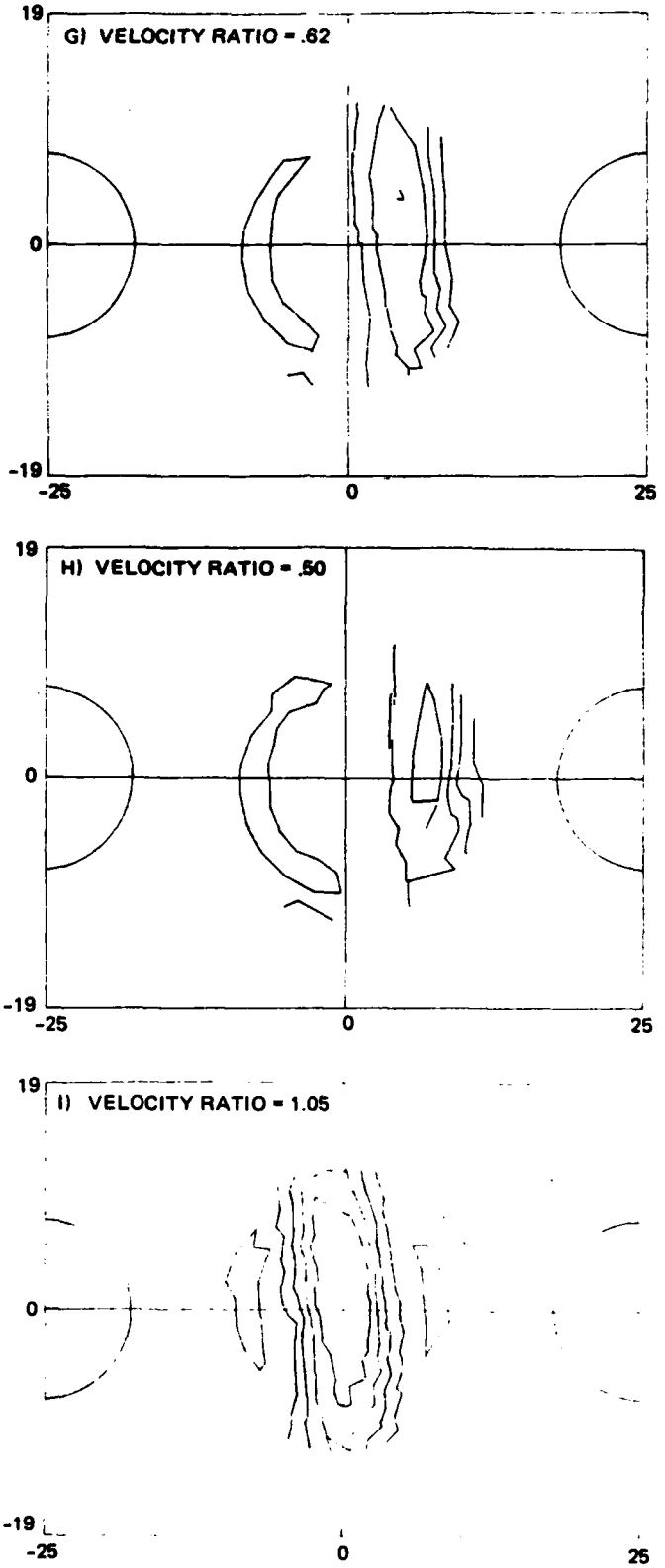


R87-3344-039(3/3)T

**Fig. 39 Ground Plane Pressure Contours for Various Source Jet Velocity Ratios (Sheet 3 of 3)**

Figures 39C through 39I show the ground pressure contours for various source jet velocity ratios. As the left jet becomes stronger relative to the right, the collision point moves towards the right. From these ground contours, it is apparent that the upwash still forms in a plane approximated parallel to the geometric symmetry plane. Some caution should be exercised when examining these data. Since the jets are relatively weaker at the collision point, the pressure rise is not as high as for the equal jet case. Since all the data are normalized by the same value, each contour line represents a higher percent of the collision pressure. Secondly, since the flow distance is longer for the stronger jet, the radial wall jet velocity profile will be relatively thicker than the equal jet height. The converse is true for the weaker jet having a thinner layer. This will have the effect of slanting the upwash away from the plane, although the maximum mean velocity of each jet will be equal at the collision point. At least for the ratios tried here, the ground pressure contours do not show any evidence of the thicker wall jet jumping over the thinner one.

# 3. CONCLUSIONS

An experimental investigation of the turbulence mechanisms in a V/STOL upwash flow field was conducted. During the course of this overall investigation a comprehensive data base has been generated for the upwash flow formed from the collision of both two-dimensional and radial wall jets. The two-dimensional data has been reported earlier. In this report, we present new measurements in a simplified geometry radial upwash. These results provide detailed data on an important class of flows where none existed. They are expected to significantly improve the computational empirical tools available for predicting V/STOL behavior near the ground.

A new flow facility was constructed to simplify the geometric complexity and interference effects found in a real V/STOL flow. The facility generates two equal radial wall jets by impinging a pipe flow onto a circular deflection plate from below the ground plane. Extensive measurements were made on the resulting radial wall jet to assure that the flow characteristics were the same as generated by more conventional means. A flow visualization technique using a laser light sheet with three-degrees of freedom mobility and video tape recordings provided good qualitative verification of the measurements.

A complete set of turbulence measurements were made in the upwash formed by the collision of radial wall jets. These measurements which were at six heights in a plane connecting the two source jets included higher moments and length scale information. Measurements were made at four heights in four planes parallel to the centerline plane. Measurements were also made along the symmetry plane and three parallel planes. Ground plane pressure contours were generated from 168 unique pressure points centered at a point between the source jets for a variety of source jet velocity ratios.

The upwash flow becomes self-preserving very rapidly. Using the collision point half velocity height as a characteristic dimension, the flow is self preserved by X/D about 4. Required linear relationships for mean velocity decay and growth rate were found at all stations across the upwash. Conservation of momentum was observed. A simple model of the upwash using a free jet equivalent may appear adequate on the symmetry plane, but under-predicts decay rate and fails completely away from the symmetry plane. The basic turbulence characteristics in the upwash formed from the collision of

radial wall jets are similar to but about 10% higher than those in a radial free jet. Comparisons suffer from lack of good radial free jet data. The most notable differences are found in the much greater mixing layer growth rate (and corresponding mean velocity decay rate) and turbulence scale. The mixing rate (0.25) is more than twice the free jet case (0.11) which is already greater than a two-dimensional free jet case (0.09). This means that there is a very large entrainment field as seen in the flow visualization. A unique feature of the entrainment is the suckdown into the collision zone rather than a tangential injection. Measurements of the length scale, flow visualization, and most obviously the intermittency show the unusually large structure of the upwash.

The higher mixing rate is explainable primarily on the basis of the head-on collision of the wall jets. This creates large turbulent eddies that involve more ambient fluid than a simple jet emanating from a slot. This is also seen by the large static pressure field at the collision point. Since the intermittency function extends more into the core of the upwash flow, time averaged turbulence energy that has approximately the same value as a free jet, must be more energetic when it is present.

## 4. ACKNOWLEDGMENTS

The flow field used in these experiments employ radial wall jets. These jets were generated in a unique way by impinging on to a deflector plate as described in Section 2.2. Much of the development of this technique for generating radial wall jets was done with the help of Richard Jenkins. Some of the upwash data taking and processing was performed by Dr. Anthony Celentano. The flow visualizing technique and the photographic digital enhancement benefit from conversations with Robert Ryan and Wayne Konopka. Thanks to George Homfeld who built much of the apparatus and made sure everything worked.

## 5. REFERENCES


1. Kalemaris, S.G., and Cea, R.A., "Effects of Technology Level on V/STOL Aircraft," AIAA Paper #77-1238, Aircraft Syst Tech Mtg, Seattle, WA, Aug 1977.

2. Kalemaris, S.G., and York, P., "Weight Impact on VTOL," SAWE Paper #1326, 38th Annual Conf of SAWE, New York, May 1979.

3. Rajaratnam, N., Turbulent Jets, Developments in Water Science, 5th ed., Amsterdam, Elsevier Scientific Publishing Co., 1976.

4. Harsha, P.T., "Free Turbulent Mixing: A Critical Evaluating Theory and Experiment," AEDC-TR-71-36, Feb 1971.

5. Kind, R.J., and Suthanthiran, K., "The Interaction of Two Opposing Plane Turbulent Wall Jets," AIAA Paper No. 72-211, AIAA 10th Aerospace Sciences Mtg, San Diego, CA, Jan 17-19, 1972.

6. Witze, P.O., and Dwyer, H.A., "Impinging Axisymmetric Turbulent Flows: The Wall Jet, The Radial Jet and Opposing Free Jets," Symp on Turbulent Shear Flows, Vol 1, Univ Park, PA, Apr 23-30, 1977.

7. Kotansky, D.R., and Glaze, L.N., "The Effects of Ground Wall-Jet Characteristics on Fountain Upwash Flow Formation and Development," AIAA Paper #81-1294, AIAA 14th Fluid & Plasma Dyn Conf, Palo Alto, CA, June 23-25, 1981.

8. Foley, W.H., and Finley, D.B., "Fountain Jet Turbulence," AIAA Paper #81-1293, AIAA 14th Fluid & Plasma Dyn Conf, Palo Alto, CA, June 23-25, 1981.

9. Jenkins, R.A., and Hill, W.G., Jr., "Investigation of VTOL Upwash Flows Formed by Two Impinging Jets," Grumman Research Department Report RE-548, Nov 1977.

10. Saripalli, K.R., "Laser Doppler Velocimeter Measurements in 3-D Impinging Twin-Jet Fountain Flows", AIAA Paper 85-4037, Oct 1985.

11. Gilbert, B.L., "Detailed Turbulent Measurements in a Two-Dimensional Upwash," AIAA No. 83-1678, AIAA 16th Fluid & Plasma Dynamics Conf, Danvers, MA, July 12-14, 1983.

12. Gilbert, B.L., "An Investigation of Turbulence Mechanisms in V/STOL Upwash Flow fields," Grumman R&D Center Report RE-667, May 1983.

13. Gilbert, B.L., "An Investigation of Turbulence Mechanisms in V/STOL Upwash Flow Fields," Grumman R&D Center Report RE-688, Aug 1984.

14. Gilbert, B.L., "An Investigation of Turbulence Mechanisms in V/STOL Upwash Flow Fields," Grumman R&D Center Report RE-708, Sept 1985.

15. Townsend, A.A., The Structure of Turbulent Shear Flow, 2nd ed., Great Britain, Cambridge Univ Press, 1980.

## 6. PUBLICATIONS


Gilbert, B.L., "Detailed Turbulent Measurements in a Two-Dimensional Upwash," AIAA No. 83-1678, AIAA 16th Fluid & Plasma Dynamics Conf, Danvers, MA, July 12-14, 1983.

Gilbert, B.L., "An Investigation of Turbulence Mechanisms in V/STOL Upwash Flow fields," Grumman R&D Center Report RE-667, May 1983.

Gilbert, B.L., "An Investigation of Turbulence Mechanisms in V/STOL Upwash Flow Fields," Grumman R&D Center Report RE-688, Aug 1984.

Gilbert, B.L., "An Investigation of Turbulence Mechanisms in V/STOL Upwash Flow Fields," Grumman R&D Center Report RE-708, Sept 1985.

Gilbert, B.L., "Turbulence Measurements in a Two-Dimensional Upwash," accepted by AIAA Journal.

Gilbert, B.L., "Turbulence Measurements in a Flow Generated by Colliding Radial Wall Jets," 10th Symposium on Turbulence, Rolla, MO, Sept 21-24, 1986. Also submitted to Experiments in Fluids.

Gilbert, B.L., "Turbulence Measurements in a Radial Upwash," AIAA No. 87-1435, AIAA 19th Fluid and Plasma Dynamics Conf, Honolulu, HI, June 8-10, 1987. Also to be submitted to AIAA Journal.

Gilbert, B.L., "New Method for Generating a Radial Wall Jet." Note in preparation.

END

7-87

DTIC